Transport of Bacteria, Viruses and a Visual Tracer in a Saturated 2-Dimensional Porous Media Model

by

Jazlyn Cauren Acosta

A Thesis Presented in Partial Fulfillment
of the Requirements for the Degree
Master of Science

Approved July 2017 by the
Graduate Supervisory Committee:

Morteza Abbaszadegan, Chair
Peter Fox
Paul Dahlen

ARIZONA STATE UNIVERSITY

August 2017

ABSTRACT

This study was designed to provide insight into microbial transport kinetics which might be applied to bioremediation technology development and prevention of groundwater susceptibility to pathogen contamination. Several pilot-scale experiments were conducted in a saturated, 2 dimensional, packed porous media tank to investigate the transport of *Escherichia coli* bacteria, P22 bacteriophage, and a visual tracer and draw comparisons and/or conclusions. A constructed tank was packed with an approximate 3,700 cubic inches (in^3) of a fine grained, homogeneous, chemically inert sand which allowed for a controlled system. Sampling ports were located at 5, 15, 25, and 25 vertical inches from the base of the 39 inch saturated zone and were used to assess the transport of the selected microorganisms. Approximately 10^5 cells of *E. coli* or P22 were injected into the tank and allowed to move through the media at approximately 10.02 inches per day. Samples were collected intermittently after injection based off of an estimated sampling schedule established from the visual tracer.

The results suggest that bacteriophages pass through soil faster and with greater recovery than bacteria. P22 in the tank reservoir experienced approximately 1 log reduction after 36 hours. After 85 hours, P22 was still detected in the reservoir after experiencing a 2 log reduction from the start of the experiment. *E. coli* either did not reach the outlet or died before sampling, while P22 was able to be recovered. Bacterial breakthrough curves were produced for the microbial indicators and illustrate the peak concentrations found for each sampling port. For *E. coli,* concentrations at the 5 inch port peaked at a maximum of 5,170 CFU/mL, and eventually at the 25 inch port at a maximum of 90 CFU/mL. It is

presumed that *E. coli* might have experienced significant filtration, straining and attachment, while P22 might have experienced little adsorption and instead was transported rapidly in long distances and was able to survive for the duration of the experiment.

ACKNOWLEDGMENTS

I would like to thank ASU for offering me the chance to work with Dr. Morteza Abbaszadegan and his team, and for providing the necessary material for my success in research. I also especially thank the ASU Technical Shop for building the laboratory tank which made this study possible. I would like to extend thanks to Stan Klonowski for the technical support and always making sure lab stayed safe and functioning, and especially for making sure the autoclaves were working.

I am sincerely grateful to Dr. Abbaszadegan for giving me the opportunity to work with him and in his lab. His environmental microbiology class was one of my favorites in my college career and Dr. Abbaszadegan was one of my favorite professors. I have enjoyed every second of my time in lab, from training to making media, and learning about the tank, frustrating as it may have been at times. If there is one thing I learned from the tank, it is that microbes never behave the way you want them to. I would like to thank Dr. Absar Alum for assisting in my training and for his continued support throughout the extent of my project. Thank you to Drs. Peter Fox and Paul Dahlen for serving as members on my committee and the time you have given me. Thank you to Paul Dahlen for allowing us to use the laboratory tank and for taking the time to answer any questions I had. All of you have made this project very enjoyable for me, and I have grown as a researcher and engineer.

Finally, I would like to thank my friends and family for always being there for me and listening to me talk about bacteria and viruses more than I should have.

TABLE OF CONTENTS

Page

Page

Page

APPENDIX Page

LIST OF TABLES

Table Page

LIST OF FIGURES

Figure Page

Figure Page

Figure Page

Figure Page

LIST OF ABBREVIATIONS

ASU	Arizona State University
ATCC®	American Type Culture Collection
bp	base pair(s)
C	microbe concentration
°C	Degrees Celsius
CDC	Centers for Disease Control and Prevention
CFT	colloid filtration theory
CFU	colony forming unit
D	Hydrodynamic dispersion coefficient
DI	deionized
DLVO	Derjaguin and Landau 1941, Verwey and Overbeek 1948
DNA	deoxyribonucleic acid
dsDNA	double stranded deoxyribonucleic acid
°F	Degrees Fahrenheit
g	gram(s)
g/L	grams per liter
gal	gallon(s)

hr(s)	hour(s)
hh:mm	Hour:Minute
in^3	cubic inches
in/day	inches per day
in/hr	inches per hour
L	liter(s)
mg/L	milligrams per liter
MHOS	micromho(s)
MHOS/cm	micromhos per centimeter
mL	milliliter(s)
mL/min	milliliters per minute
µm	micron(s)
mm	millimeter(s)
nm	nanometer(s)
ND	not detected
NOP	National Organic Program
NTU	Nephelometric Turbidity Unit
PBS	phosphate buffer saline
PFU	plaque forming unit

RPM	revolutions per minute
S	attached microbe concentration
t	time
TDS	Total Dissolved Solids
TNC	too numerous to count
TSA	Tryptic Soy Agar
TSB	Tryptic Soy Broth
U.S.	United States
WHO	World Health Organization
x	distance
v	interstitial microbe velocity
ρ_b	dry bulk density
ε	bed porosity
5L	5 inch, Left Side
5R	5 inch, Right Side
15L	15 inch, Left Side
15R	15 inch, Right Side
25L	25 inch, Left Side
25R	25 inch, Right Side

35L	35 inch, Left Side
35R	35 inch, Right Side

INTRODUCTION

Motivation

The study of subsurface ecosystems has illuminated the common detection of *E. coli* bacteria and other pathogenic or virulent microorganisms in surface and groundwater systems. *E. coli* has been observed to experience rapid movement and transport in soil. The ability these bacteria have to persist in reclaimed and recharged water can lead to microbial contamination of groundwater aquifers and water sources. Some bacteria and bacteriophages can be used as indicators of fecal contamination and the presence of other harmful pathogens. To prevent or retroactively repair the environmental disturbance this contamination creates, remediation technologies and risk assessment techniques must be developed, and can only be successful if microbe-facilitated pollutant transport potential can be accurately predicted and modeled. An improved understanding of the mechanisms which influence the transport of bacteria can aid in constructing a realistic model which can then be applied to bioremediation. Packed-media column experiments can be used to assess the influence of biological factors on bacterial transport and deposition kinetics. Water flow in porous media is dependent on water content and subsurface geochemistry. Understanding physicochemical filtration, or removal, of bacteria which passes through the media can help to understand survival and predict travel distances. An improved mechanistic understanding of the factors influencing microbial transport and fate can help to access susceptibility of groundwater systems to establish treatment goals for safe groundwater.

Significance

As a result of agricultural practices and various waste disposal techniques, microbial contamination has had a direct influence on the availability of safe and reliable water sources. Scarcity of safe drinking water has fueled the desire to close the knowledge gap concerning the transport of bacteria. Ingestion of contaminated water has led to major outbreaks of water-borne diseases and deaths. Aquifer recharge practices are also known to introduce the potential of contaminant mobility and transport into groundwater sources. Recharge is a hydrologic process through which water moves from surface water down to groundwater and is the primary way through which water enters an aquifer. This can be done naturally, through surface infiltration, or through an engineered system. Potential contaminant transport presumably increases with recharge rates. A more accurate ability to predict the transport of microorganisms and pollutants can help the community address public health concerns and risks and proactively work to reduce contamination. Improved techniques and practices can decrease water scarcity and water-borne disease outbreaks.

Goals of this Study

The outcomes from this research can help to construct a more cohesive and comprehensive model of the overall transport of bacteria and viruses in groundwater systems. The project will specifically investigate pilot-scale transport of *E. coli,* P22, and a Fluorescein dye in a 2-dimensional granular porous media packed model. Fluid phase concentration of suspended microbes within the model will help to produce bacterial breakthrough curves which can be used to draw conclusions of mean transport behavior,

survival, and travel distances of the targeted microorganisms. Overall, the yielded data can be used in furthering the understanding of microbial transport in saturated media and possibly help in the future development of bioremediation technologies to address public health concerns and the scarcity of safe drinking water. The data will be used to determine microbial indicators' transport as a model for pathogenic microorganisms and accessing the risk and threat of contamination to groundwater.

The main objective of this study was to investigate the transport of *E. coli,* P22 and a visual tracer in a 2-dimensional porous media model. This study was developed to accomplish the following:

- To use Fluorescein dye to understand 2-dimensional; flow characteristics of the tank and determine if the arrival of the bacteria and bacteriophage could be predicted.
- To investigate the 2-dimensional transport of *E. coli.*
- To investigate the 2-dimensional transport of P22.

LITERATURE REVIEW

Mechanisms of Transport of Microbes through Soil and Aquifers

Pathogenic bacteria and viruses which cause disease have been detected in ground and surface receiving waters, and a considerably large portion of water-borne disease outbreaks in the U.S. are attributable to contaminated water sources. Groundwater is susceptible to pathogen contamination, which has been found to originate from sewage outbreaks and septic tanks, infiltration of rain flowing through landfills, artificial recharge of aquifers using treated sewage water, and land application of wastewater (Corapcioglu and Haridas, 1984). The threat of contamination is heightened because lab and field investigations have observed that microorganisms have the ability to survive for long periods of time and travel significant distances through soil, both vertically and horizontally (Abu-Abshour et al., 1994). The source of contamination is primarily fecal pollution and agricultural practices such as land application of sewage or disposal of waste. The most important documented microorganisms when it comes to transport in groundwater and soils are *E. coli* and the hepatitis virus, Norwalk virus, echovirus, poliovirus, and coxsackievirus. Because of the threat of disease outbreaks, understanding microbial transport and the mechanisms which affect it are essential in addressing public health and environmental concerns.

Along with microorganisms being carried with bulk flow, there are several modes of microbial transport through soil, including:

> Movement in water films due to motility of the microorganisms... microbial growth which may contribute to microbial transport; and… microbial dispersion

through soil by water movement. The latter mode is independent of microbial motility or growth (Abu-Abshour et al., 1994).

The mechanisms can be divided into physical, biological, and geochemical processes.

The physical processes which act as mechanisms for transport include convection, advection, and hydrodynamic dispersion (Abu-Abshour et al., 1994). Microbes that are carried with the bulk flow are governed by the velocity of the carrying fluid, which is known as advection, also equal to the product of hydraulic conductivity and the hydraulic gradient divided by the porosity, and is considered a passive mode of transport. Dispersion is the spreading of microorganisms during transport. Dispersion is further divided into two processes: diffusion and mechanical mixing, and can be influenced by the mobility of the microbes. Diffusion is the spreading of microorganisms as a result of a concentration gradient, and plays a large role as a mechanism of transport for smaller particles like viruses. Diffusion is considered negligible in bacterial transport, since mechanical mixing plays a larger role. Mechanical mixing can occur from the fluid velocity distribution within pore space, or from variations in true pore velocities among channels of different surface roughness and size. Convergence or divergence of pore channels can also cause mixing. Fractures and macropores encourages mixing and results in more effective dispersion. “Dispersion results in dilution of contaminant pulses, attenuation of concentration peaks and arrival of contaminants well ahead of the time expected on the basis of average velocity of water flow” (Abu-Abshour et al., 1994).

The physical processes which act as mechanisms for transport also include filtration, adsorption/desorption and sedimentation, and primarily hinder microbial

transport (Abu-Abshour, et. al, 1994). There are three mechanisms for filtration which can prevent microbes from flowing through a pore. Surface, cake or vacuum filtration occurs when microbes are too large to penetrate soil, and therefore accumulate on the surface of the soil, affecting soil permeability. This occurs when the ratio of soil grain diameter to microbes is less than 10. Straining occurs when the ratio is between 10 and 20, and "particles whose sizes are 1 and 10 μm were removed by both cake and straining mechanisms at the surface" (Abu-Abshour et al., 1994). A particle in suspension flowing with the bulk fluid may be larger than pore opening, and thereby accumulate on soil grain surfaces (Corapcioglu and Haridas, 1984). Straining is reported to be a main factor in the attenuation of bacterial transport through soil, and considered negligible for viruses based on their smaller size (Corapcioglu and Haridas, 1984).

Another mechanism is physical chemical or physicochemical filtration, which occurs when the ratio is greater than 20, and can exceed 1000. Physicochemical filtration depends mainly on microbe-media collision and attachment, which is when microbes are removed from the bulk fluid and attach to sediment grain surfaces, and is more predominant in bacterial transport and negligible for viral transport. It can be irreversible, meaning no detachment, or reversible, in which case both equilibrium and kinetic mechanisms are applied (Tufenkji, 2007). The general transport equation is known to be:

$$\frac{\partial C}{\partial t} = -v\frac{\partial C}{\eth x} + D\frac{\partial^2 C}{\partial x^2} \quad [1]$$

Where D is the hydrodynamic dispersion coefficient, C is the microbe concentration in aqueous phase, x is distance, t is time and v is microbe velocity. Incorporating removal of

microbes brings the equation for one-dimensional, homogeneous, saturated porous medium to:

[2] $$\frac{\partial C}{\partial t} + \frac{\rho_b}{\varepsilon}\frac{\partial S}{\partial t} = D\frac{\partial^2 C}{\partial x^2} - v\frac{\partial C}{\partial x}$$

Where ρ_b is dry bulk density, ε is bed porosity, and S is attached microbe concentration. The degree of filtration can be dependent on volume of water, rate of irrigation and on time delay between inoculation and irrigation (Abu-Abshour et al., 1994). Detachment can be illustrated in bacterial breakthrough curves by estimating the measured amount "tailing;" long tailing is indicative of very slow release, which can contribute to and increase bacteria travel distances.

Adsorption, another attenuating mechanism, is reversible and is when substances collect on an interface in aqueous suspension. It can be influenced by pH, temperature and ions in the medium. Adsorption plays a primary role in viral transport due to their small size. "The normally negatively charged bacterial and viral surfaces are strongly adsorbed by anionic adsorbents" (Abu-Abshour et al., 1994). Desorption is when adsorbed microbes detach from soil surfaces and release into fluid and can be readsorbed. A study conducted by Wellings et al, observed in a well that viruses initially adsorbed into soil particles were undetectable, but after heavy rainfall they desorbed in the water and were then detected (Abu-Abshour et al., 1994). Physical adsorption occurs due to van der Waals forces; the adsorbed particle is "not affixed to a specific site at the surface but, rather, is free to undergo translational movement within the interface (Corapcioglu and Haridas, 1984). Viral adsorption is primarily governed by electrostatic double-layer interactions and these van der Waals forces.

Sedimentation is more important for larger size and density particles and is the gravitational deposition onto soil grain surfaces. The density of the particles needs to be more than the fluid and when the flow allows for settling rather than movement. Since bacteria and viruses are small and neutrally buoyant, sedimentation usually does not occur (Abu-Abshour et al., 1994).

The biological processes which act as mechanisms for transport include microbial growth, inactivation or death and is influenced by pH, fluid composition, temperature, nutrient availability, environmental conditions and competition with other organisms (Abu-Abshour et al., 1994) (Tufenkji, 2007). Inactivation can affect suspended and attached microorganisms. Viral inactivation is very sensitive to temperature. However, the dynamics of populations of microbes is difficult to quantify and can be unpredictable, as the effect of these parameters on the rate of inactivation is still unclear (Tufenkji, 2007). The intrinsic characteristics of microbes also inherently governs their transport. Motile microorganisms have experienced migration in chemical gradients, which is known as chemotactic migration, moving away from high chemical concentrations. Chemotactic migration is not a factor of viral transport (Abu-Abshour et al. 1994).

Classical Filtration Theory and Microbial Indicators. Colloids are particles between 100 nm and 100 μm, which includes *E. coli* bacteria. The colloid or classical filtration theory (CFT) is when attachment of microbes to soil surfaces is irreversible. The CFT is most applicable when the system of interest is initially free of microorganisms, is considered steady-state, and is described by the attachment or collision efficiency, where dispersion is negligible. The theory posits that bacteria which

are colloids will experience less removal/deposition during the transport process as compared to larger microbes, since they have lower probability of collision with porous media grain surfaces. Less removal translates to faster transport of the bacteria (Abbaszadegan et al., 2011). Deposition of colloids is primarily controlled through two processes: "(1) Transport of colloid to porous media grain surfaces and (2) colloid-surface interaction, which is governed by the forces that may allow or prevent direct attachment of the colloid with the grain surface" (Abbaszadegan et al., 2011). Interaction forces which act between colloids and media are traditionally estimated on contributions from electric double layer and van der Waals interactions. The DLVO theory (Derjaguin and Landau 1941, Verwey and Overbeek 1948) posits that the electric double layer is repulsive with like-charged colloid and grain surfaces, with distance of strength of this repulsion being inversely related to ionic strength of the solution. The van der Waals interaction is attractive for most surfaces and can be considered independent of the chemistry of the solution. Both interactions decay as the distance between colloids and surfaces increase "such that can der Waals attraction may greatly dominate at small separation distances, electric double layer repulsion may dominate at intermediate separation distances, and van der Waals attraction may slightly dominate at greater separation distances" (Abbaszadegan et al., 2011). Energy barriers are defined as those repulsion interactions between colloids and grain surfaces; the presence of these barriers, however, has been shown to not necessarily prevent colloidal deposition (Abbaszadegan, 2011).

The filtration theory can also be applied to the use of viruses as an indicator organism. Viruses generally have relatively low inactivation rates and cannot reproduce rapidly in conditions absent of suitable hosts in groundwater. CFT implies that bacteria will undergo less removal than viruses due to greater diffusion of the viruses to the sediment grain surfaces, though viruses have been known to associate with grain particles that encourages their removal during transport. Studies conducted yielding results in agreement with the theory have observed stronger attenuation of viral indicators as compared to bacterial indicators (Gupta et al., 2008). However, this theory may not always be realistic for environmental conditions, because viruses are still detected in groundwater systems. Studies have observed significant retention of colloids near the given source or inlet, including homogeneous porous media systems (Gupta et al., 2008). Repulsion between colloid and collector surfaces is not predicted in the CFT, and this type of repulsion is common in the environment, which may account for the differences in results and theory (Gupta et al., 2008).

Factors Which Influence Transport of Microbes through Soils and Aquifers

Groundwater composition, flow path, subsurface chemistry and the type of media through which bacteria and viruses travel have immense effects on their behavior and survival. *E. coli* has been found to travel greater distances in certain types of soil, even under similar conditions. Their movement can also be very fast, which is attributed to the presence of macropores within the media, creating preferential flow, observed in both lab and field studies (Abu-Abshour et al., 1994). Preferential flow is unevenly distributed and is much more rapid than matrix flow, which is relatively slow with a more even

distribution in comparison. Interactions between soil, bulk fluid, and microorganisms also control behavior and transport. Table 2.1 summarizes major factors which affect the survival of bacteria and viruses in soil (Abu-Abshour et al., 1994). Table 2.2 summarizes factors which affect their movement.

Table 2.1 Factors Affecting the Survival of Bacteria and Viruses in Soil

	Factor	Comments
1.	Microorganisms and their physiological state.	
2.	Physical and chemical nature of receiving water.	
–	pH	– Shorter survival time in acidic soils (pH 3–5) than in alkaline soils.
–	Soil water content	– longer survival time in wet soils and during times of high rainfall.
–	Organic matter content	– Increased survival and possible growth when sufficient amount of organic matter is present.
–	Texture and particle size distribution	– Finer soils especially clay minerals and humic substances increase water retention by soil which increases survival time.
–	Temperature	– Longer survival at lower temperature.
–	Availability of nutrients	– Increases survival times.
–	Adsorption properties	– Microorganisms appear to survive better in sorbed state.
3.	Atmospheric conditions	
–	Sunlight	– Shorter survival time at the soil surface.
–	Water (vapor and precipitation)	– Same as in (2) above.
–	Temperature	– Same as in (2) above.
4.	Biological interactions	
–	Competition from indigenous microflora	– In sterile soil, survival is increased.
–	Antibiotics	– Many microorganisms cannot survive in the presence of antibiotics
–	Toxic substances	– Same as antibiotics
5.	Application method	
–	Technique	
–	Frequency of application	
–	Organism density in waste material	

Table 2.2 Factors Affecting Movement of Microorganisms in Soil

1.	Soil physical characteristics
	– Texture
	– Particle size distribution
	– Clay type and content
	– Organic matter type and content
	– pH
	– Pore size distribution
	– Bulk density
2.	Soil environment and chemical factors
	– Temperature
	– Soil water content
	– Soil water flux
3.	Chemical and Microbial factors
	– Ionic strength of soil solution
	– pH of infiltrating water
	– Nature of organic matter in waste effluent solution (concentration and size)
	– Type of microorganism
	– Density and dimensions of the microorganism
	– Presence of larger organisms
4.	Application method
	– Soil drying between applications
	– Time of application (winter, spring)

Size and morphology of microorganisms affect their transport through soil; a study conducted by Gerba and Bitton found that when *E. coli* bacteria and a coliphage were injected simultaneously into an aquifer, the larger *E. coli* experienced more rapid movement than the phage (Abu-Abshour, et al., 1994). However, some studies have reprorted that there is preferential removal of long, rod-shaped cells (Tufenkji, 2007). It has also been found that grain size of the media, cell size, and ionic strength are important factors influencing bacterial transport within porous media and aquifers.

"Interactions between mineral grains in the aquifer and bacterial cells influenced adhesion of cells to the mineral grains, and hence play an important role in determining the movement of bacteria through saturated porous media (Abu-Abshour et al., 1994). In saturated porous media, the composition of the bulk fluid carrying the bacterial cells is important; modifying the chemical composition can enhance or hinder transport. Finally, plants and other organisms can affect the survival of microorganisms in soil by creating predation and competition from other bacteria, and may even enhance mixing of microorganisms within soil. Sterilization is therefore important when studying the behavior of microbes. Since the survival and transport of bacteria through soil is so highly dependent on myriad factors, it is important to establish context when investigating transport so that the parameters are understood, or to limit the number of variable parameters.

E. coli Background Information

Characteristics and Morphology. *Escherichia coli* bacteria, also known as *E. coli*, belong to the family of Enterobacteriaceae (*Escherichia coli*: pathogen safety data sheet- infectious substances, 2012). Bacteria in this family all have four distinctive features: they ferment glucose, reduce nitrates to nitrates, are oxidase negative, and are motile (Sanders & Brophy-Martinez, 2007). *E. coli* bacteria are the most significant species among this genus and remain prevalent because they pose a potential, opportunistic pathogenic threat to humans. The bacteria are gram negative, rod shaped, measure approximately 0.5 μm (microns) in width by 2 μm in length, are facultative anaerobic, non-spore forming and are usually motile with peritichous flagella, and do not produce

enterotoxins (*Escherichia coli*: pathogen safety data sheet- infectious substances, 2012). The bacillus, rod shape can be illustrated in Figure 2.1.

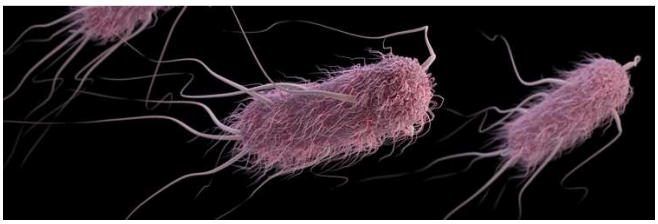

Figure 2.1 *E. coli* Bacteria

Source: Centers for Disease Control and Prevention. (2015, November 06). Retrieved 2017, from https://www.cdc.gov/ecoli/images/ecoli-1184px.jpg

***E. coli* as a Microbial Indicator.** *E. coli* are a subgroup of fecal coliforms which exist in large quantities in the intestines and feces of animals and humans, meaning that the presence of the bacteria in a drinking water sample indicates the presence of fecal contamination and a greater risk for exposure to pathogens (Washington State Department of Health). Consumption of drinking water with confirmed fecal coliforms or *E. coli* can pose health risks. Some types of *E. coli* are not harmful and are essential elements within human intestinal tracts, but some strains are pathogenic and can lead to a wide range of infections depending on the group of bacteria. As a fecal coliform and a subgroup of total coliforms, *E. coli* is a type of bacteria which is commonly used as an indicator of the presence of pathogens and fecal pollutions. Since coliforms are facultatively anaerobic and are found within intestines, their presence in a water sample usually means that there are other infectious or pathogenic microorganisms also present. Therefore, coliform

concentrations are used as an official standard for drinking water. They are present in high concentrations in surface waters, easy to identify, and are easily detected. Tests which show a positive result for total coliforms will be followed by a confirmation test, which is done to determine if there are fecal coliform, like *E. coli*, also present in the sample. If so, this is said to prove fecal contamination (Abbaszadegan et al., 2011). The only stipulation is that they have the ability to survive in saturated sediments may not always indicate recent fecal contamination.

Transmission. *E. coli* bacteria is primarily transmitted through consumption of contaminated foods or fecal contamination of water, along with fomites (World Health Organization, 2016). The infectious dose is estimated to be 10^6 organisms with an incubation period between 6 to 48 hours (Centers for Disease Control and Prevention, 2015). Though ozone can physically inactivate the bacteria and it is sensitive to high temperatures, *E. coli* can survive between 1.5 hours and 16 months after excretion from host, and has been found to specifically survive for months in manure and water trough sediments (*Escherichia coli*: pathogen safety data sheet- infectious substances, 2012).

E. coli Presence in Soils and Aquifers

Though contamination of water is more well known as a mode of transmission, there is increased awareness of soilborne *E. coli*, which may be more ubiquitous than has been previously assumed. Viable populations of the bacteria have been isolated in tropical and subtropical soils, though there is limited information on environmental presence, survival and growth of *E. coli* in sediments and soils (Ishii et al., 2006). A study conducted by Ishii et al on temperate soils form Lake Superior watersheds found

that the population density of soilborne *E. coli* was subject to seasonal variation, with greater cell densities of up to 3×10^3 CFU/g soil in summer to fall and ≤ 1 CFU/g soil during winter to spring. DNA fingerprints of these samples showed that the soilborne strains were unique to specific soils and locations, which indicates that the strains had naturalized within the soil microbial community. These strains were found to have the capability to grow to high cell densities in nonsterile soils when incubated at 30 or 37°C, and to survive for more than 1 month. It was also found that counts were higher after tidal events, which could mean that the bacteria "can grow in riverbank soils and move back into water by erosion. Based on these results, soil and sand should perhaps be thought of as both a sink and a source of *E. coli* for waterways" (Ishii et al., 2006). The presence of the bacteria has led to increased desire for an understanding of microbial survival in soils and groundwater.

P22 Background Information

Characteristics and Morphology. P22 is a bacteriophage which is a part of the *Podoviridae* family that infects the *Salmonella typhimurium* bacteria (Casjens, 2000). P22 is commonly used as a model phage when investigating the transport and behavior of bacteriophages. Bacteriophages, also known as phages, are viruses which infect and invade bacterial cells and not human cells; they are "metabolically inert in their extracellular form (the 'virion'), and they reproduce by insinuating themselves into the metabolism of the host" (American Society for Microbiology). Bacteriophages have also been known to be potential indicator organisms, and "have been used as surrogates to study the removal of human enteric viruses" (Abbaszadegan et al., 2011). The presence

of bacteriophages in a water sample is usually an indicator of the presence of other infectious microbes and possible fecal pollution. Bacteriophages as indicators are a popular method due to their relationship with waterborne infection, ease of detection and efficient, low cost procedures. They are used to identify the presence of sewage contamination, measure efficiency of wastewater treatment plants, and to model how similar or related viruses and bacteria may exist in the environment, as they exhibit behaviors similar to other pathogens under both natural environment conditions and water treatment processes (Abbaszadegan, 2011).

P22 can be used as a model bacteriophage when investigating transport and transport behavior, thereby assessing both general phage behavior and the efficiency of phages as indicator organisms. P22 is a temperate dsDNA phage; the dsDNA phages are tailed phages whose genomes are molecules of linear double stranded DNA and are relatively large in comparison to most viruses at 50,000 bp (base pair) (American Society for Microbiology). It is a lamboid phage as it carries control of gene expression regions and early operons that are similar to the phage lambda. P22 has a virion morphology with an icosahedral virion head of about 60 nm (nanometer) in diameter with a very short tail, shown in Figure 2.2.

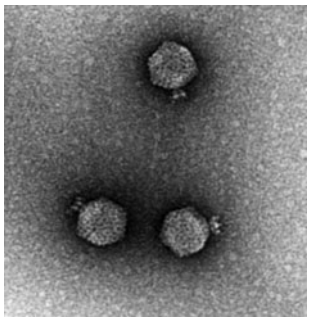

Figure 2.2 Bacteriophage P22

Source: Casjens, S., & Lenk, E. (2000, August 15). Electron micrograph of bacteriophage P22. Retrieved 2017, from https://www.asm.org/division/m/foto/P22Mic.html

P22 was the first phage shown to have the ability to perform generalized transduction, a process in which DNA is transferred to another cell by the virus; "P22 builds a protein 'procapsid' first and then places the DNA chromosome within this preformed container" (Sherwood, 2000). P22 infects *Salmonella* by binding to the O-antigen, which is part of the outer membrane, and the virion's tail fiber protein cleaves the O-antigen chain so it many penetrate the membrane of the host (Sherwood, 2000). Upon infection, P22 can grow through a lytic or lysogenic growth pathway, controlled primarily through the multiplicity of infection. In the lytic cycle, the series of viral genes that are expressed produce several hundred progeny virions per cell, released around one hour after infection through lysis of the host. In the lysogeny life cycle, "the phage chromosome integrates into the host chromosome, and expression of the phage structural genes is suppressed. The integrated phage is called a prophage, which is replicated and passed to the daughter cells during cell division" (P22 Bacteriophage (Molecular

Biology)). Once cells have been processed on media and plaques are produced, each plaque can illustrate the pathway that was taken. Figure 2.3 shows two different types of plaques formed from P22 infected *Salmonella enterica.* The cloudy plaque is a lysogenic plaque, made from lysogenizing of the cells. "The cloudy centers are due to the growth of lysogenic cells containing quiescent prophage DNA. A ring of lysis surrounds the cloudy center because low-level release of virus particles from lysogenic cells results in infection and lysis of surrounding cells" (Slonczewski & Foster, 2011). The clear plaques are lytic cells made from phages capable of lysis of cells.

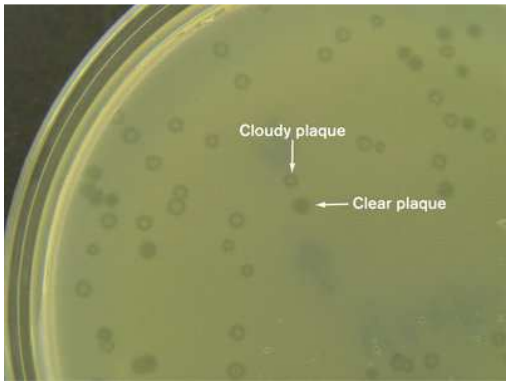

Figure 2.3 Lytic vs. Lysogenic P22 plaques

Source: Slonczewski, J. L., & Foster, J. W. (2011). *Microbiology: An Evolving Science*(2nd ed.). Retrieved from http://www.wwnorton.com/college/biology/microbiology2/ch/10/etopics.aspx

Once bound to the host membrane, P22 moves laterally in repeated binding and release cycles until it can locate a second receptor, at which point the binding is irreversible and the dsDNA is injected into the bacterial cell in a linear fashion. It then

"circularizes by homologous recombination between the terminal redundancy regions, yielding a circular dsDNA that represents a single copy of the phage genome" (P22 Bacteriophage (Molecular Biology)). Figure 2.4 shows an electron micrograph of a *Salmonella typhimurium* cell infected by P22 approximately 30 minutes after injection.

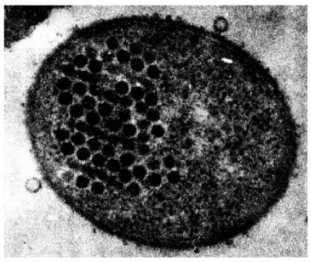

Figure 2.4 P22-Infected *Salmonella typhimurium* Cell

Source: P22 Bacteriophage (Molecular Biology). (n.d.). Retrieved 2017, from http://what-when-how.com/molecular-biology/p22-bacteriophage-molecular-biology/

Modeling Microbial Transport in Packed Media Models

Studies conducting investigations on the roles of the physical, geochemical and biological factors which govern microbial transport, along with testing the influencing factors, are traditionally done in bench and pilot-scale 1-dimensional packed porous media columns, or 2-dimensional tanks/models. Model particles are selected to assess the transport of similar microorganisms; if the model particles are successfully transported, then the mechanism of transport for similar microbes also exists. Viral transport investigations usually employ bacteriophages as model particles, and viral removal in granular filtration is performed in packed beds of quartz sand, natural sediments and glass

beads, and bromide tracers (Tufenkji, 2007). It has been found that viral attachment kinetics are generally governed by electrostatic interactions like van der Waals forces, which attract or repulse objects with unlike electric charges (Tufenkji, 2007). Bacterial transport is sometimes more difficult to model, based on the physical heterogeneity of the media through which bacteria moves and the inherent complexity or understanding all the different parameters.

The most common way of investigating microbial transport kinetics is through the measurement of suspended, fluid-phase concentrations at intermittent travel distances. Though this method may not be sufficient enough to identify to the detailed extent each mechanism plays in transport, it can be utilized to develop predictive models for behavior in natural and engineered systems. More extensive studies pair fluid phase concentrations with spatial distribution of retention of microbes to understand deposition behavior. Mathematical models use simplified forms of the advection dispersion transport equation ([1]). Most commonly, microbe removal is modeled as being solely governed by attachment to grain surfaces.

A study conducted by Silliman et al. sought to model bacterial transport through media where hydraulic conductivity varied as a 2-dimensional, log distributed, 2nd-order stationary, exponentially correlated random field. The investigation involved 2 strains of bacteria and was designed to determine the transport and retention of the strains in the packed columns, and to compare the transport of the bacteria with a chemical tracer. Microbial concentrations were determined via sampling from septa and bacteria attached to sand that was removed during destructive sampling was determined. Bacterial

breakthrough curves were produced and bacterial abundance on the solid phase was illustrated. The results showed that retention was greatest at the surface of the column, and that the bacteria breakthrough curves had significant time tailing and slow release. The number of bacteria on the solids showed high spatial variability, especially when compared to fluid phase suspension. The results showed that the behavior of the bacteria was consistent with the visual tracer, and that the tracer was able to predict the arrival and peak concentration times of the bacteria. The study demonstrated that the bacteria breakthrough behavior was also consistent with those observed with homogeneous media and select observations from the field (Silliman et al., 2001).

Nathalie Tufenkji compiled a report in 2007 detailing common strengths and weaknesses that studies make when modeling microbial transport in porous media. The report exhibited similar trends with other successful studies on the same subject like the Silliman et al. study. For example, it has been found in other studies that the observed breakthrough curves for bacteria are comparable to the breakthrough of the tracers, a conclusion that Silliman et al. reached in their interpretation of their results (Tufenkji, 2007). Tufenkji also reported that microbial growth and inactivation are difficult to predict and that methodologies fail to account for possible inactivation over long time periods when analyzing their results. Tufenkji also reported that fluid-phase particle concentration alone is inadequate in identifying the significant mechanisms of transport. It was stressed that the most accurate models must consider fluid-phase concentration in conjunction with the measurement of microbe spatial distribution in the solid phase. This

represents a more sensitive measure of filtration behavior than just the profile of suspended microbes. A more accurate prediction of microbe migration can be made when the distribution of deposition rates is considered.

Other model studies have studied viral and bacterial transport and compared the results. Viruses have been added to water and applied to soil columns and it has been found that saturated conditions yield much higher subsequent concentrations of viruses (Gerba et al., 1989). It was concluded that unsaturated flow encourages inactivation of viruses, and saturated flow yields very little adsorption to the soil. The stability of bacteriophages makes them useful in transport kinetic studies; most bacteriophages can survive for long periods of time in saturated soil conditions, and some studies have reported negligible inactivation even for 72 hour durations with rapid transport (Powelson et al., 1990). Bromide tracers are often used in the modelling of bacteriophage transport in porous media. A 2008 study investigated the use of P22 as a tracer in complex surface water systems, and found that P22 can be valuable and more accurately model viruses, especially when compared to tracers which may not adequately describe suspended colloid behavior (Shen et al., 2008). The study was conducted in a 40 km long section of a river, and reported P22 inactivation rates of 0.12-0.25 log reduction per day, with the highest rates found in areas with high suspended solid concentrations, low dissolved organic carbon, and high clay content. It was concluded that the results from the P22 model could be used to examine arrival times and expected concentrations of viral pathogens deposited from untreated sewage (Shen et al., 2008). A more recent study conducted this year by Park et al. compared the transport of bacteriophage to bacteria,

including *E. coli*. The results demonstrated that phages are transported through more easily than bacteria under saturated flow conditions. Bacteria log removals in the soil columns ranged from 0.44 to 1.72, while log removals of bacteriophages were between 0.01 and 0.13 (Park et al., 2017).

Studies involving the transport of bacteria and *E. coli* specifically have found that the probability of groundwater contamination is significantly increased, implicated by the common behavior of *E. coli* to flow through soil macropores. In doing so, the bacteria bypass "the adsorptive or retentive capacities of the soil matrix," thereby avoiding filtration and increasing travel distance (Smith et al., 1985). Soil structure is also found to extend or shorten transport, and columns prepared from repacked soil were more effective filtration systems for bacteria than intact soils. Smith et al. found that as water input flowrate increased, recovery of *E. coli* in the effluent also increased, which reinforced the suggestion of macropore flow (Smith et al., 1985). Bradford et al. studied the behavior in quartz sands of different sizes and flowrates, and found that concentration curves became more asymmetric as sand size decreased, and finer sands (240 to 150 μm) tended to produce higher effluent concentrations at higher velocities. Coarse sands and high flow rates resulted in less deposition and decreasing concentration with depth, and fine sand with low flow rates resulted in greater deposition and "nonmonotonic deposition profiles that exhibited a peak in retained concentration. This deposition peak occurred nearer to the column inlet for finer-textured sands and at low flow rates" (Bradford et al., 2006). The results indicated that straining was the dominant mechanism of deposition for *E. coli*. The study conducted one investigation with a fine sand of 240

μm, with a flowrate of 14.4 in/day, and a porosity of 33%, and found low recovery of *E. coli* in the effluent and that most of the *E. coli* was retained on the sand, as illustrated in Table 2.3, where

$$q = velocity$$

$$\varepsilon = porosity$$

$$L_c = column\ length$$

$$T_o = pulse\ duration$$

$$M_{eff}, M_{sand}, M_{total}$$

$$= Mass\ percentage\ recovered\ in\ effluent, sand, and\ total, respectively$$

Table 2.3 Recovery of *E. coli* at Different Sand Grain Sizes and Flowrates

d_{50}, μm	q, cm min^{-1}	ε	L_c, cm	T_o, min	M_{eff}	M_{sand}	M_{total}
710	0.031	0.334	12.53	150.0	78.2	23.7	101.9
710	0.114	0.357	12.97	75.0	82.4	3.2	85.6
710	0.196	0.330	12.45	37.5	80.1	8.5	88.6
360	0.024	0.341	12.66	150.0	54.3	43.2	97.5
360	0.099	0.333	12.50	75.0	73.0	5.8	78.8
360	0.196	0.348	12.80	37.5	68.1	10.4	78.5
240	0.026	0.324	12.35	150.0	9.2	85.0	94.2
240	0.097	0.332	12.49	75.0	42.1	30.4	72.5
150	0.017	0.334	10.00	150.0	0.3	95.9	96.2
150	0.102	0.341	12.66	75.0	13.2	52.4	65.6
150	0.177	0.350	10.00	37.5	47.0	33.8	80.8

Source: Bradford, S. A., Simunek, J., & Walker, S. L. (2006). Transport and straining of E. coli O157:H7 in saturated porous media. *Water Resources Research,42*(12). doi:10.1029/2005wr004805

The study also provided pictures of the *E. coli* strain deposited within the sand grains at grain junctions, small pores, and/or pore constrictions due to straining. They found that attachment is not the dominant mechanism for *E. coli* deposition in fine sand based on the retention on the solids.

MATERIALS AND METHODS

Preparation and Packing of Soil Tank

The pilot-scale studies were conducted using a stainless-steel tank enclosed with acrylic windows, and reinforced with steel braces to protect from fracturing. The tank was previously built by the ASU Engineering Technical Service shop. The tank is 72 inches tall, 24 inches wide, and 4 inches deep, and has sampling ports intermittently on the surface of the acrylic windows, accessible by removable septa. The front of the tank was previously divided into a 2 inch by 2 inch visual grid, where each cube represents a 2 inch by 2 inch area of sand. Before packing, the tank was filled with water and disinfected with a solution of approximately 1 cup of Great Value bleach to 5 gallons tap water. After filling and adding the bleach solution, the tank was allowed to sit for around 5 hours, then fully drained, dried, and flushed with tap water 4 times. Approximately 3,744 in^3 of dry Quikrete© Mesh Fine Silica Sand was added in roughly 12 inches lifts, tamped on the surface of the sand and on the tank sides with a rubber mallet for consolidation. The sand was added until it reached a height of 39 inches within the tank, and was topped with a 3 inch gravel layer to weight the sand. The final packed tank was filled from the bottom up with a solution of around 1 cup of Great Value bleach to 5 gallons of water to disinfect the sand layer for about 5 hours; subsequent to bleaching, the tank was flushed with tap water four times. The final saturation of the tank was from the bottom to minimize trapped air. When saturated, a pool volume of average 1.5 inch height would accumulate above the gravel layer. A schematic of the packed tank can be seen in Figure 3.1, and a photo of the tank itself can be seen in Figure 3.2.

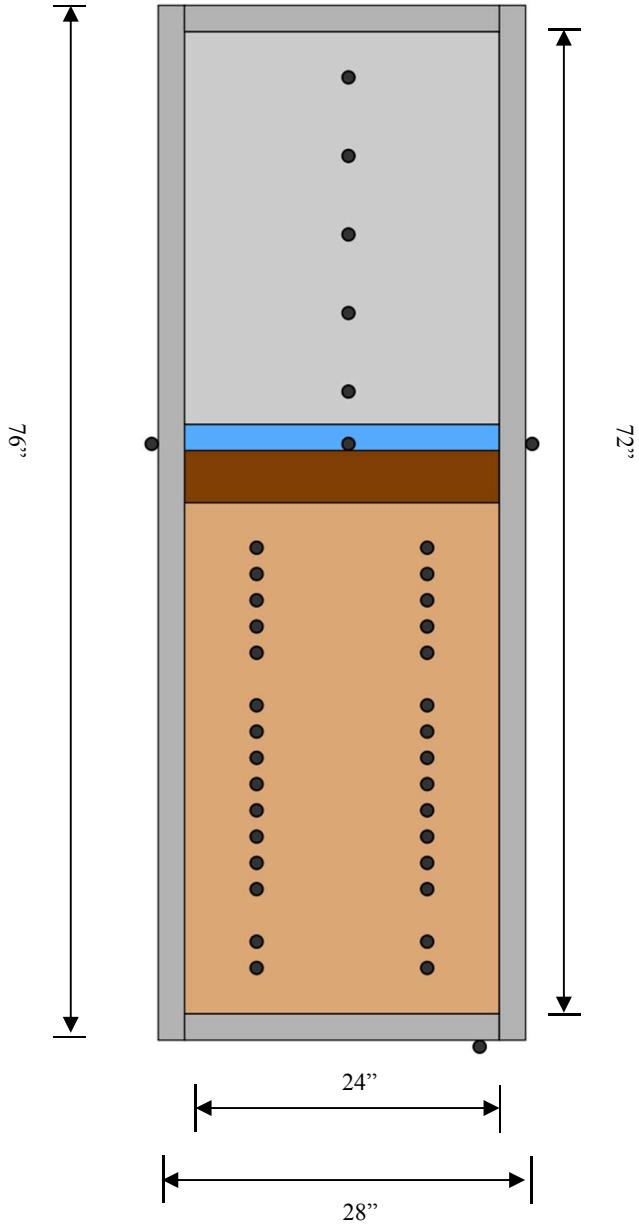

Figure 3.1 Tank Schematic with Sampling Port Configuration(left)

Figure 3.2 Photo of Tank (right)

Pictured in both figures on the bottom right of the tank is the inlet/outlet from the bottom of the tank (Figure 3.3) that was connected to a Cole-Parmer Masterflex® (Vernon Hills, IL) peristaltic pump which controlled the flow rate through the tank (Figure 3.4). A size 15 Cole-Parmer pump head was used, along with size 15 Cole-Parmer Masterflex Norprene (Vernon Hills, IL) tubing pictured in Figure 3.4, and a generic ¼ inch polyethylene white tubing pictured in Figure 3.3. Whether they were considered inlets or outlets depended on the direction of flow in the tank. This inlet/outlet releases or draws water from a single inlet and stainless-steel diffuser that spans the width of the tank, a schematic of which can be seen in Figure 3.5.

Figure 3.3 Inlet/Outlet Point at Bottom of Tank

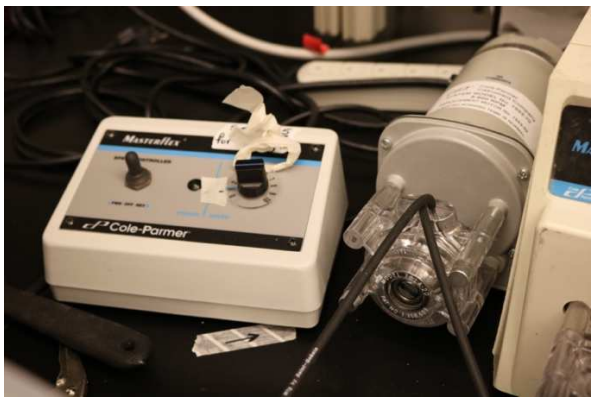

Figure 3.4 Peristaltic Pump Which Controls Tank Flowrate

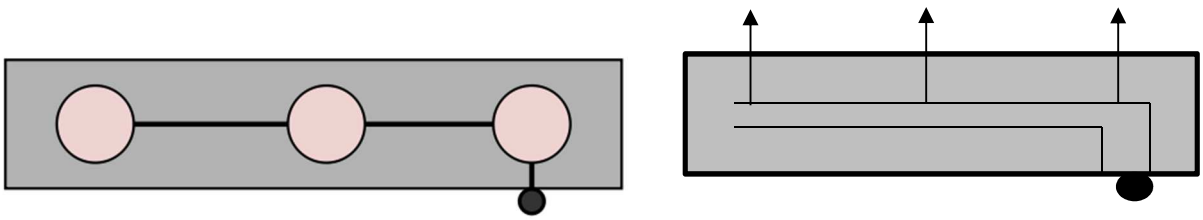

Figure 3.5 Schematic of Inlet/Outlet Point Along Bottom of Inside of Tank

Media Properties

The media selected to pack the tank was Quikrete© (No. 1961) Mesh Fine Silica Sand, the data sheet for which can be found in Appendix A. The sand is among the predominant size range associated with the U.S. sieve number #30-#70 (0.6-0.2 mm) (Commercial Grade Sands: Product Nos. 1961, 1962, 1963). The ANSI grit size is 60, and based off Table 3.1 found in Appendix B, is contained specifically to sieve size 0.01 mm, with a grain size of 250 μm (Grit Sizes – ANSI, 2017). The homogeneous layer of sand has a porosity of 30%, and allows for closely controlled sizing and particle size distribution. Considering all the factors which affect transport, like grain size, texture, chemical interactions etc., this sand was chosen to provide a very homogeneous, controlled medium through which the microorganisms would travel through to reduce variable factors.

The sand is hard, chemically inert, and has a high boiling point which can be attributed to strength of the bonds between the atoms. It is made primarily of silicon dioxide (SiO_2) and is non-reactive. Comparatively, the silica sand grit size is 60 and based off Table 3.1 found in Appendix B, the grain size is 250 μm, while the *E. coli* cells are around 2 μm in length, and the P22 phage is usually 0.06 μm in diameter. Figure 3.6

gives an idea of the differences in sizes between the media, bacteria, and phage. The ratio of soil grain diameter to *E. coli* cell size is between 125 and 500, and is around 4,100 for P22.

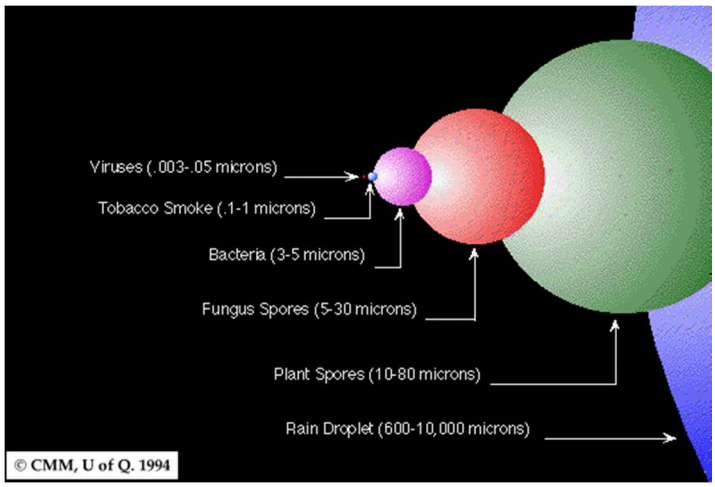

Figure 3.6 Micron Size Chart

Source: Hartford University. (2001, November). Retrieved 2017, from http://uhavax.hartford.edu/bugl/microbe.htm

The porosity of the sand was determined by placing a measured volume of 1000 mL of the media in a beaker, consolidated by tapping. Water was slowly added down one side of the beaker to avoid air entrapment. The beaker was filled until the liquid was level with the top of the sand. The volume of water that was added was approximately 312 mL. A porosity of 31% was determined by taking the ratio of the volume of liquid to the volume of sand. The high porosity, well sorted state and presumably high permeability of the sand may reduce adhesion/cohesion of water molecules to grain particles and allow for efficient movement through the media.

Determining and Setting Flow Rate through Packed Tank

The flow rate in the tank was controlled by a peristaltic pump and the corresponding pump head and tubing sizes connecting the tank to the inlet/outlet reservoirs. The desired flowrate was one between 10 to 12 in/day. The speed on the pump was adjusted and the flowrate coming directly from the tubing was measured. This measured flowrate was used to estimate the flowrate through the sand in the tank. The tank was filled with a total volume of 3,744 in^3 of sand with 31% porosity, which means that there was approximately 2,583.4 in^3 (11.18 gal) of packed volume, and approximately 1160.6 in^3 1160.64 (5.02 gal) of void volume. The flow rate directly from the pump was measured to be 3.39 mL/min, which resulted in a calculated flowrate through the sand of approximately 0.42 in/hr or 10.02 in/day, which met the desired flowrate. The calculations to determine this flowrate were completed as follows:

$$\frac{0.0034\ L}{min} \times \frac{gal}{3.78\ L} = \frac{8.98 \times 10^{-4} gal}{min} \times \frac{60\ min}{hr} \times \frac{24 hr}{day}$$

$$= \frac{1.29\ gal\ fluid}{day}\ through\ column$$

This result indicates that approximately 1.29 gal of fluid would travel through the tank in one day at the measured flowrate.

$$\frac{5.02\ gal\ void\ volume}{\frac{1.29\ gal}{day} fluid} = 3.89\ days$$

It would take 3.77 days for the fluid to fill the entire void volume within the tank, or to move through 39 inches of sand, which is the height of the volume of sand.

$$\frac{39\ in}{3.89\ days} \times \frac{day}{24\ hrs} = 0.42\frac{in}{hr}\ \ or\ \ 10.02\frac{in}{day}$$

Therefore, it is estimated that it takes 1 hour for the fluid to move through 0.42 inches of sand within the tank, which translates to the fluid travelling through 10.02 inches of sand per day.

Once the flowrate had been adjusted to 10.02 in/day, the speed on the pump was locked and all pilot-scale studies were performed at the determined flowrate. Groundwater velocities are usually modelled as slow seepage through pore spaces, and velocities of 1 foot per day is considered high rate of movement. However, when groundwater pollution is involved, flowrates are usually found to be higher, and the EPA reports that groundwater and contaminants can move rapidly through macropores and fractures. The flowrate selected for this study is most representative of this kind of flow.

Fluorescein Dye-Tracer Test through Tank

A model study was performed to investigate the transport of a visual tracer, Fluorescein Dye (Fisher Chemical A833-100), through the porous media within the tank at the determined flowrate. The dye-tracer test was conducted from January 26, 2017 to February 2, 2017. The inlet reservoir, a carboy with 20 L of water, was dosed with the dye at a concentration of 2 g/L. At lower concentrations, the dye could be detected from sampling at the ports but was not visible on the media. Once the dye had entered the tank, and the pattern could be observed on the media, the estimated distance travelled was recorded over time. The results were used to create a template sampling schedule for the detection of *E. coli* and P22.

Preparation of Microbial Stocks

E. coli and P22 were targeted for microbial analysis. *E. coli* bacteria and P22 phage were used for the transport modeling experiments in the pilot-scale model study. *Salmonella* was used as the host cell for the P22 phage. The primary objective of the pilot-scale model study was to investigate and model the transport of *E. coli* and P22 through the soil media under recharge conditions.

***E. coli* culture.** The *E. coli* (ATCC® 25922™) strain was acquired from the ATCC. This strain of *E. coli* is of serotype O6, biotype 1 and originates from a clinical sample and is "a commonly used quality control strain" (Minogue et al., 2014). It is a very well-characterized strain. The frozen stock was thawed and placed on a TSA plate via the streak plate method, and incubated in a 37°C incubator for 24 hours. With the streak plate method, A sterile wire, called an inoculating loop, is used to pick up bacteria from a sample and spreading it over the surface of an agar plate, attempting to pull the isolated bacteria away from others so that it can multiply and increase the number of isolated colonies without being mixed with a different type of organism. After 24 hours, a colony was extracted from the TSA plate and inoculated in a tube containing 5 to 7 mL of TSB and placed in a 37°C incubator for 24 hours to prepare an overnight culture. After the first 24 hours, reculturing was performed by transferring 0.1 mL into a fresh tube of 5 to 7 mL of TSB, repeated every 24 hours for up to a week to keep the culture viable. The stock was serially diluted and analyzed via spread plate method on TSA to determine the concentration of the solution and/or Brilliance™ *E. coli/Coliform* Selective Agar

(Oxoid). Cells could be injected to the tank influent reservoir, which would then be sampled at time 0 and compared with samples collected at a later time.

***Salmonella* culture.** The *Salmonella typhimurium* (ATCC® 19585™) strain was acquired from the ATCC. The frozen stock was thawed and placed on a TSA plate with a sterile inoculating loop via the streak plate method, and incubated in a 37°C incubator for 24 hours. After 24 hours, a colony was extracted from the TSA plate and inoculated in a tube containing 5 to 7 mL of TSB and placed in a 37°C incubator for 24 hours to prepare an overnight culture. After the first 24 hours, reculturing was performed by transferring 0.1 mL into a fresh tube of 5 to 7 mL of TSB, repeated every 24 hours for up to a week to keep the culture viable. To ensure that the bacteria was in the growth stage for the assay of the samples collected from the tank, 0.1 mL of the culture was transferred into the necessary amount of TSB needed for the given sample 3 hours before performing the assay.

P22 culture. The P22 (ATCC® 19585-B1™) strain was acquired from the ATCC. The stock was propagated used the double agar layer method; following incubation after the double agar layer assay, the phage was collected by adding to 10 mL of 1X phosphate buffer saline (PBS) to the surface of the plate and left at room temperature for 1 hour. The supernatant was collected and centrifuged at 4 °C at 8000g for 15 min. The resultant pellet was discarded and the supernatant was stored at 4 °C (Abbaszadegan et al., 2007). The stock was serially diluted and analyzed to determine the concentration of the solution.

Sample Collection Method

Samples were collected from the 5 in, 15 in, 33 in, and 35 in sampling ports, along with the reservoir. The sampling port names correspond to the distance from the tank inlet. For example, the 5 inch sampling port is located 5 vertical inches from the inlet. On the sand layer, there are sampling ports on the left side of the tank and the right side, located the same vertical distance from the inlet. Therefore, there is a left 5 inch port and a right 5 inch port, referred to as 5L and 5R, respectively, for each port (5 in, 15 in, 25 in, 33 in, 35 in). Samples from the right ports and left ports, at the same vertical location, would be collected simultaneously. A 25G 5/8 inch needle was placed directly in the middle of the port septa, and a flush volume of 5 mL was allowed to drip from the needle to prevent suction within the tank. After flushing, 5 mL was collected as the sample. Following collection, a syringe was used as a stopper, as seen in Figure 3.7.

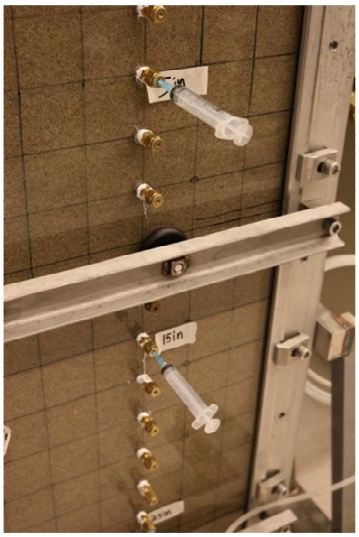

Figure 3.7 Right Side Sampling Ports

Sample Processing and Assay Methods

***E. coli* analysis by Spread Plate Technique.** When detecting *E. coli* presence in the tank, the samples were analyzed using spread plate technique on Brilliance agar selective media. Spread plating takes the diluted solution and spreads it on the surface of the agar plate, and then the petri dish is incubated for 24 hours. The samples were individually vortexed to obtain a homogeneous distribution immediately before being transferred onto the surface of the agar. Enumerated *E. coli* appeared as purple bacterial colonies after incubation and were counted and recorded to measure bacterial growth.

Preparation of Brilliance media. Brilliance agar media (OXOID CM1046) is a selective media for *E. coli*, which was used for the detection of *E. coli* in the tank samples. 28.1 g of Brilliance agar base was added to a flask containing 1000 mL of distilled water and boiled on a hot plate. Mixing was performed using a magnetic bar set at 200 RPM. Once the media was mixed and boiled, it was cooled to 50°C and aseptically dispensed into petri dishes in quantities of 15 mL per petri dish. The plates were left at room temperature until solidified; once solidified, the plates could be used immediately or be bagged, labelled by name and date, and stored in a 4°C refrigerator for future use. For the pilot-scale model studies, all samples containing *E. coli* were assayed within 30 minutes of collection.

P22 detection by Double-Agar Layer Technique. When detecting P22 presence in the tank, the samples were analyzed using the double-agar layer technique with TSA and TSB media. The underlay (bottom agar) was a TSA plate and the overlay

(top agar) was a TSB media with added agar or agarose which would allow for solidification after the assay had been completed. 5 mL of the top agar was stored in sterile test tubes and before the assay, the appropriate number of test tubes were sterilized by autoclaving and placed in a 45°C water bath. 1 mL of the tank sample, serially diluted as needed containing P22, vortexed immediately before use, was poured into the top agar test tube, followed by 1 mL of *Salmonella* culture. The mixture was then poured directly onto the surface of the bottom agar plate. In addition, positive and negative control plates were made to check the health of the host cell and of the top agar. The positive control was made by pouring 1 mL of the *Salmonella* host into the 5 mL of top agar, mixing, and pouring directly onto the surface of the bottom agar. The negative control was made by pouring the 5mL top agar alone onto the bottom agar. The plates were left for 30 minutes to 1 hour to solidify and placed in a 37°C incubator for 24 hours, at which point bacterial growth could be recorded. Samples from the tank were assayed within 1 hour of collection.

Preparation of TSA media. TSA (Soybean-Casein Digest Agar) was used for the propagation of the microbial stocks and for the detection of the P22 phage in the tank samples as the bottom agar. 40 g of the medium was suspended in a flask with 1000 mL of DI water and boiled on a hot plate. Mixing was performed using a magnetic bar set at 200 RPM. Once the media was mixed and boiled, it was sterilized by autoclaving at 121 °C, cooled to 50°C and aseptically dispensed into petri dishes in quantities of 15 mL per petri dish. The plates were left at room temperature until solidified; once solidified, the plates could be used immediately or be bagged, labelled by name and date, and stored in

a 4°C refrigerator for future use. For the pilot-scale model studies, all samples containing P22 were assayed within 2 hours of collection.

Preparation of TSB media. Bacto ™ TSB (Soybean-Casein Digest Medium) were used for the propagation of the microbial stocks and to make the top agar used in the double agar layer method. 30 g of powder was suspended in a flask with 1000 mL of nano-pure water and boiled on a hot plate. Mixing was performed using a magnetic bar set at 200 RPM. Once the media was mixed and boiled, it was sterilized by autoclaving at 121 °C. The TSB could then be used or stored for later use. Top agar was made by adding agarose base to the TSB medium. TSA has 15 g of agar, and since top agar is to have half, 7.5 g of agar was added to TSB to make top agar. The top agar was dispensed in quantities of 5 mL into sterile test tubes and could be used immediately or stored at 4°C for later use.

Investigation of Survival of *E. coli* with and without Chlorine Neutralization

To investigate the ability of *E. coli* in chlorinated versus dechlorinated water, a carboy was filled with 20 L of tap water which still had its chlorine residual, and 4 mL of *E. coli* stock was injected. Another carboy was filled with 20 L of tap water, but 1 mL of Sodium Thiosulfate ($Na_2O_3S_2$) was also added along with the injected 4 mL of *E. coli* stock to neutralize the chlorine in the tap water. Samples from each carboy were collected after mixing via magnetic bar for approximately 30 minutes and analyzed using the spread plate technique, and incubated for 24 hours at 37°C at which point bacterial growth could be observed. It was found that without the addition of sodium thiosulfate, the chlorine residual in the tap water was high enough to kill and prevent the injected *E.*

coli cells from growing. Figure 3.8 and 3.9 show the results on Brilliance media after incubation. With chlorine neutralization, the *E. coli* cells were able to grow and purple bacterial colonies were enumerated. Without chlorine neutralization, the *E. coli* cells were unable to grow. Based on these results, all pilot-scale studies were performed with dechlorinated water.

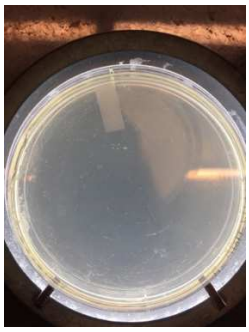

Figure 3.8 *E. coli* Growth without Chlorine Neutralization by Sodium Thiosulfate

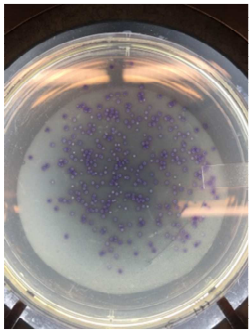

Figure 3.9 *E. coli* Growth with Chlorine Neutralization by Sodium Thiosulfate

Investigation of Survival of Microbes over Time

P22 Stability. To investigate the stability of P22 over time, a carboy was filled with 20 L of dechlorinated water and 1 mL of the P22 stock was injected to reach a desired concentration of 10^5 CFU/mL. Samples were taken at various intervals after

injection and processed to obtain bacterial numbers. Table 3.2 shows the stability or potential growth P22 in the reservoir after a given time period. These results illustrated that P22 is more stable and was able to survive in the reservoir, though it did experience die-off.

Table 3.2 Survival of P22 in Reservoir Over Time

Time after injection (hrs)	Concentration (Average PFU/mL)
0	$\geq 10^5$
36	29,000
65	6,930
85	1,300

Pilot-Scale Investigations of Saturated Spiked Model

A model study in a tank was initiated to evaluate the transport and behavior of the bacteria and bacteriophage under laboratory conditions. The studies were performed under saturated conditions (wet packing). During the duration of the experiment, the tank was fed with a constant stream of tap water from the City of Tempe. Table 3.3 lists City of Tempe tap water quality parameters, which could be considered similar to those found in the influent water to the tank. To account for the chlorine residual in the feed water, Sodium Thiosulfate was added to the reservoir along with the microbial stocks to neutralize the chlorine for all experiments at 1 mL to 20 L. Table 3.4 lists the theoretical detection limit for the microorganisms, which does not include the detection of dead cells.

Table 3.3 City of Tempe Tap Water Quality

Constituent	Units	Range	Typical Values
Chlorine Residual	mg/L	0.0-2.0	0.64
Hardness	mg/L	220-420	244
Alkalinity	mg/L	130-370	172
pH	-	6.9-7.7	7.3
Turbidity	NTU	-	<0.07
TDS	mg/L	360-1200	658
Coliform	-	ND-1.5%	ND
NO_3	mg/L	-	6.4
Temperature	°F	70-80	74
Conductivity	MHOS/cm		
Chloride	mg/L	60-420	215

Table 3.4 Microbial Detection Limits by Analysis Method

Microorganism	Detection Limit	Analytical Method
E. coli bacteria	1 cell/mL	Spread Plate Method
P22 phage	1 cell/mL	Double Agar Layer Method

Spiked Dose *E. coli* Experiments, Pressure Flow. The *E. coli* spiked dose transport experiments were performed between November 30, 2016 and March 24, 2017. For these first experiments, the tank was subject to pressure/injected flow, against gravity, controlled by the peristaltic pump. A schematic for the pressure flow set up is shown in Figure 3.10. Water from the reservoir, pictured on right, was pumped through the inlet at the bottom of the tank, and discharged from an outlet approximately 45 inches

from the inlet, pictured on the left side of the tank (Figure 3.11). Between each experiment, the tank was flushed once or twice with bleach, then flushed with tap water 3 to 4 times to wash out any remaining chlorine. At first, flushing was done at the same flowrate as the experiments and would take several days for one complete flush, but after several runs the *E. coli* bacteria was seemingly not able to reach the sampling ports. This was attributed to the formation of biofilms within the tank. To account for this, flushing was done at very high flowrates, and one flush could be completed in under 2 hours. After flushing, background concentrations were taken before the start of each experiment to ensure that no bacteria were present.

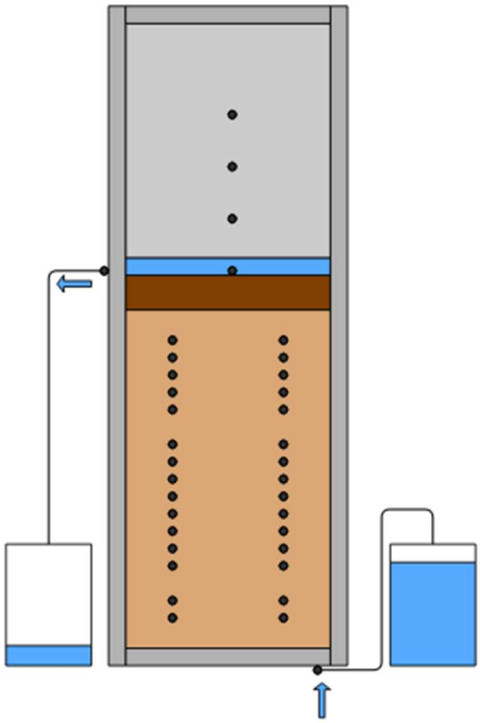

Figure 3.10 Injected Flow Set-Up Schematic

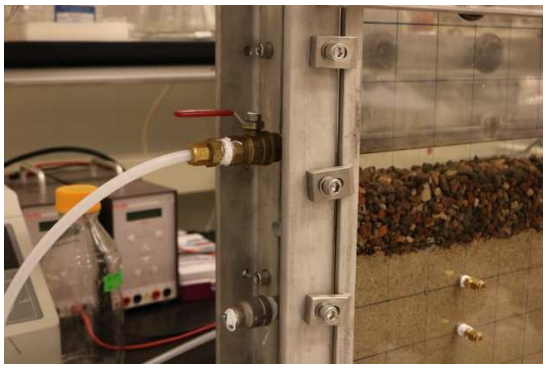

Figure 3.11 Discharge Outlet for Pressure Flow Experiments

Broth cultures of *E. coli* were grown for 24 hours and approximated at about $5 \times 10^8\ CFU/mL$. A desired inlet concentration of 10^5 CFU/mL, therefore, required a dose of 4 mL stock, injected directly into the reservoir which contained 20 L of dechlorinated water. The reservoir, containing a magnetic bar, was placed on a stirring plate and was constantly mixed throughout the duration of the experiment. The calculations to determine the required dose were performed as follows:

$$C_1V_1 = C_2V_2$$

$$\frac{10^5\ CFU}{mL} \times 20{,}000\ mL = (2x10^9 CFU)$$

$$5 \times 10^8 \frac{CFU}{mL} \times V = 2 \times 10^9\ CFU$$

$$\frac{2 \times 10^9 CFU}{5 \times 10^8 CFU/mL} = 4\ mL\ stock$$

It takes approximately 4 days to replace the entire volume of water within the Tank, so samples were taken periodically up to 105 hours after injection.

Spiked Dose *E. coli* Experiments, Gravity Flow. The *E. coli* spiked dose transport experiments under gravity flow were performed between April 10, 2017 and April 28, 2017. The tank was subject to gravity flow, controlled by the peristaltic pump. A schematic for the pressure flow set up is shown in Figure 3.12. Water from the reservoir, directly to the right of the tank, was pumped through an inlet on the right-hand side approximately 45 inches from the bottom of the tank, above the gravel layer. An outlet at the same vertical position but on the left-hand side of the tank discharged the water back into the reservoir to allow for a constant cycling to promote a homogeneous mixture feed into the tank. The feed was allowed to flow through the sand layer where it was eventually discharged at the outlet. Similar to the pressure flow experiments, flushing with and without chlorine bleach was completed between experiments. The same dosage was used for both pressure and gravity flow, and sampling was done up to 105 hours after injection.

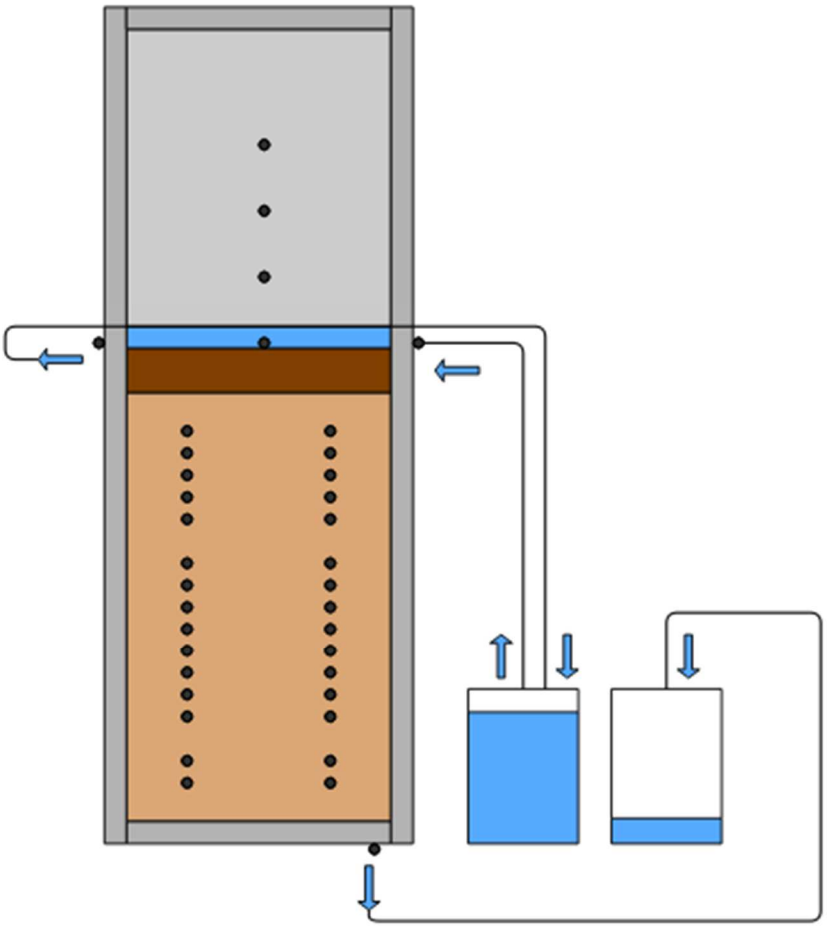

Figure 3.12 Gravity Flow Set-Up Schematic

Spiked Dose P22 Experiments, Gravity Flow. The P22 spiked dose transport experiments under gravity flow were performed between May 17, 2017 and June 8, 2017. The tank was subject to gravity flow, controlled by the peristaltic pump, as in Figure 3.13. Flushing with and without bleach was completed between each experiment. Cultures of P22 were propagated and stored at 4°C and approximated at about 1×10^9 PFU/mL. A desired inlet concentration of 10^5 PFU/mL, therefore, required

a dose of 2 mL stock, injected directly into the reservoir which contained 20 L of dechlorinated water. The reservoir, containing a magnetic bar, was placed on a stirring plate and was constantly mixed throughout the duration of the experiment.

Data Analysis

Microsoft Excel 2016 software was used to perform data analysis and prepare graphical representation of data from the model studies in the tank.

RESULTS AND DISCUSSION

Dye-Tracer Test Patterns and Transport

The model study investigating the transport of the visual tracer under pressure flow was performed to give a visual illustration of the flow patterns within the tank and to provide a basis for sampling for bacteria. After injection, the migration of the Fluorescein dye was tracked and the time of the arrival at the sampling ports was recorded. This helped to produce a template sampling schedule to determine if the bacteria and phage could be predicted by the tracer. Pictures of the dye pattern over time were taken and some of these can be seen in Figures 4.1 through 4.6 below, and more can be found in Appendix E:

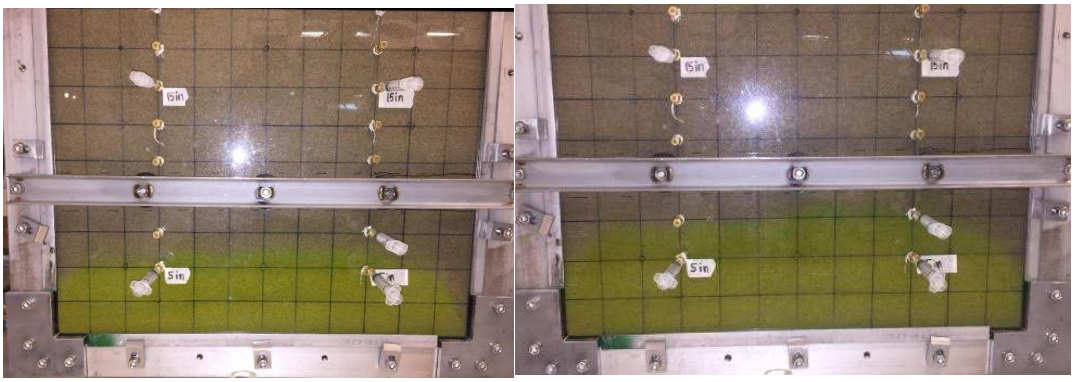

Figure 4.1 Dye Pattern on Media 14 Hours after Injection (left)

Figure 4.2 Dye Pattern on Media 18 Hours after Injection (right)

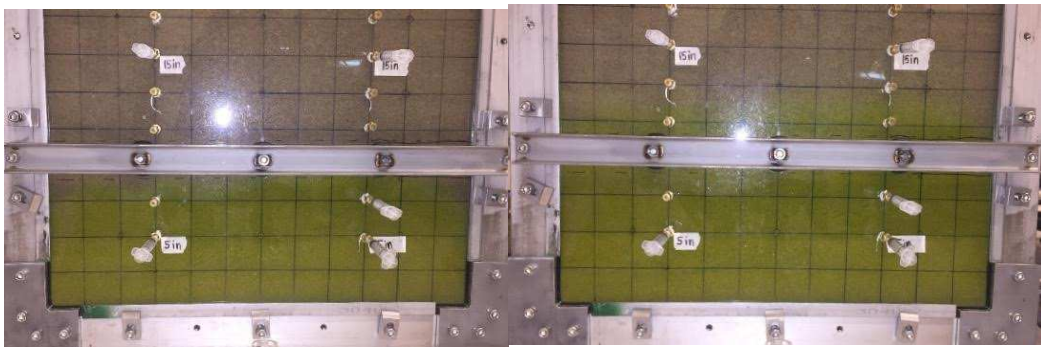

Figure 4.3 Dye Pattern on Media 22.5 Hours after Injection (left)

Figure 4.4 Dye Pattern on Media 34 Hours after Injection (right)

Figure 4.5 Dye Pattern on Media 49.5 Hours after Injection (left)

Figure 4.6 Dye Pattern on Media 66 Hours after Injection (right)

As illustrated in these figures, the dye pattern seemed to show that the rate at which the tracer moved was consistently higher on the right side as compared to the left. In fact, the right side dye pattern seemed to be about an inch above the left side at any given time, or about half an hour ahead. Figure 4.7 shows the estimated distance travelled by the tracer over time from the pictures of the dye pattern.

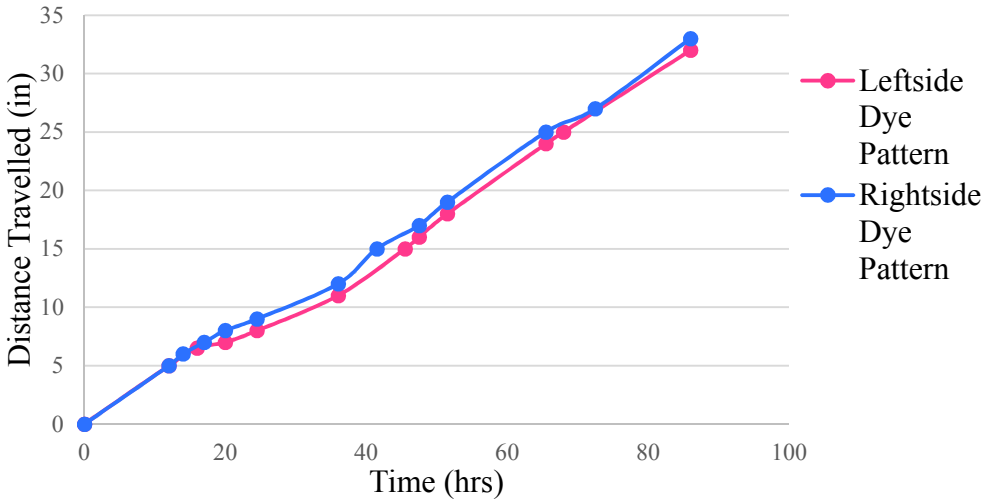

Figure 4.8 Transport of Fluorescein Dye Over Time

A linear trend line produced equations which could be used to predict the arrival of the tracer at a given time or distance. Equation 3 is for the right side, and Equation 4 below is for the left side.

[3] $$Distance\ Travelled = 0.3726\ (Time) + 0.0915$$

[4] $$Distance\ Travelled = 0.365\ (Time) - 0.415$$

These equations show that the dye travel rate was found to be 0.36 in/hr for the left side, and 0.37 in/hr for the right side. The equations were used to create predicted arrival times for each sampling port, a summary of which can be seen in Table 4.1.

Table 4.1 Summary of Predicted Arrival Times at Each Port

Sampling Port	Predicted Arrival Times (hr:min)	
	Left	Right
5 in	14:48	13:42
15 in	42:12	40:30
25 in	69:36	67:18
35 in	97:00	94:12

Based on these results, for example, it would take 14 hours and 48 minutes for the tracer to arrive at the 5L port, and 13 hours and 42 minutes for the tracer to arrive at the 5R port. A sampling schedule template was also made, summarized in Table 4.2, where an "✓" indicates that a sample should be taken at that time.

Table 4.2 Sampling Time Schedule

Time After Injection (hrs)	Sampling Port			
	5 in	15 in	25 in	35 in
10	✓	-	-	-
15	✓	-	-	-
35	✓	✓	-	-
40	✓	✓	-	-
65	✓	✓	✓	-
70	✓	✓	✓	-
85	✓	✓	✓	✓
105	✓	✓	✓	✓

Limitations. There are some inherent limitations which accompany the dye-tracer results. The equations which predicted the arrival at the sampling ports were based on pictures taken of the tank and the visible dye pattern on the media, and not on fluid phase concentrations of the dye at the sampling ports. Therefore, the actual breakthrough of the dye is difficult to ascertain from the pictures, so the times presented are merely estimations.

Spiked Dose *E. coli* Experiments

Preliminary Injection and Sampling, Pressure Flow. Before completing the dye-tracer test, an initial run was performed with an injection of *E. coli* under pressure flow, with an initial reservoir concentration of approximately $1.8 \times 10^5\ CFU/mL$. Sampling was not done based on the predicted arrival times found from the dye, and was only done once per port. The results are illustrated in Figure 4.9. The x-axis represents time after injection, and the sampling port the sample was taken at is shown above the data.

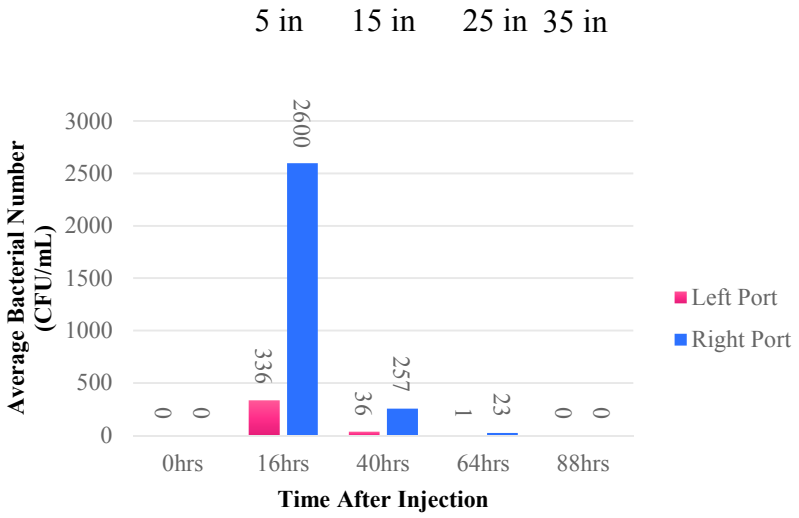

Figure 4.9 Transport of *E. coli* Over Time, Pressure Flow

Background concentrations before the start of the experiment showed that there was no *E. coli* detected. The concentration of *E. coli* in the tank after injection was consistently higher in the samples eluted from the right side sampling ports. For both sides, the concentrations of the samples taken reached their peak after 16 hours, found at the 5 inch port, with a dramatic decline at the next sampling time. The *E. coli* was either not able to reach the 35 inch port or died before sampling was completed. These results could not provide any conclusive evidence about bacterial breakthrough, so the dye-tracer test was performed.

***E. coli* Breakthrough Based off of Dye-Predicted Arrival Times, Pressure Flow.** After completing the dye tracer test, another *E. coli* model study in the tank was performed, with an initial reservoir concentration of $2.2 \times 10^5\ CFU/mL$. For this experiment, sampling was done solely based off the dye-predicted arrival times shown previously in Table 4.1. Samples were taken twice at each port: the predicted arrival time for the left side and the predicted arrival time for the right side. Figure 4.10 below summarizes these results. The x-axis represents time after injection, and the sampling port the sample was taken at is shown above the data. Breakthrough for this experiment is defined as the first time the indicators were detected in sampling, and not necessarily the actual first arrival of the indicators at the ports.

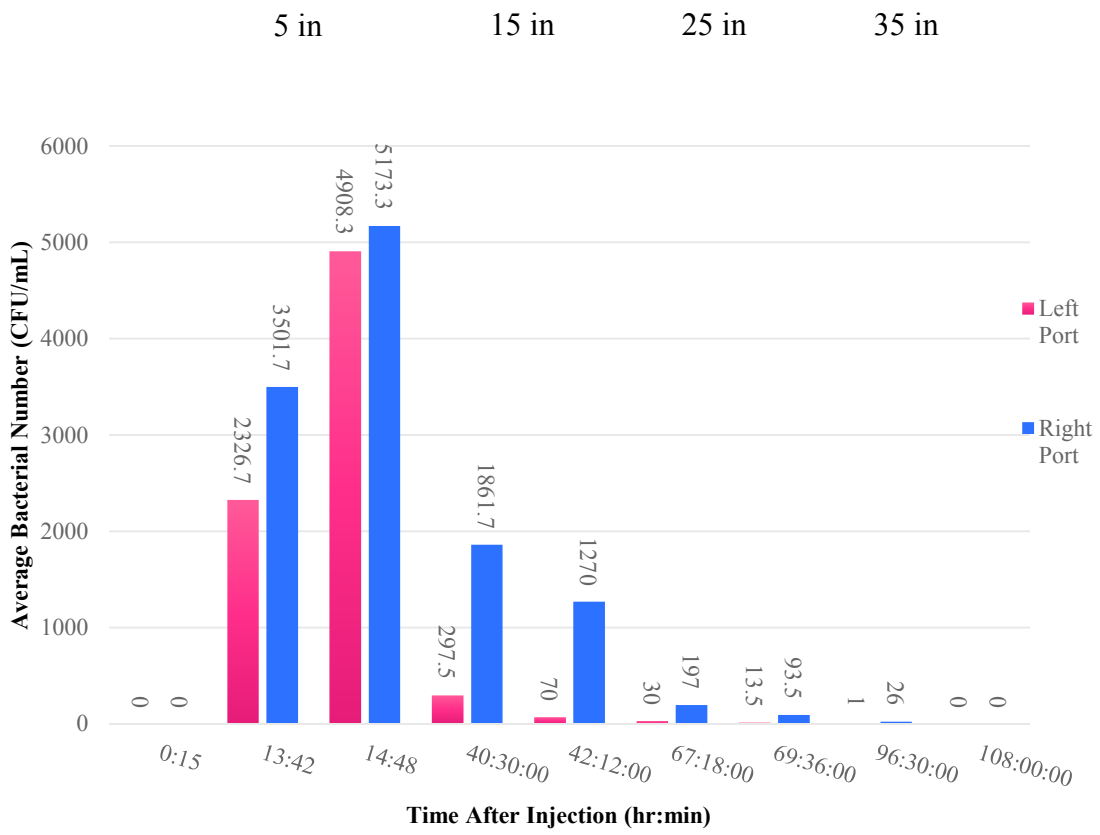

Figure 4.10 Transport of *E. coli* Over Time, Pressure Flow

Background concentrations before the start of the experiment showed that there was no *E. coli* detected in the tank. The concentration of *E. coli* in the tank after injection was consistently higher in the samples eluted from the right side sampling ports. Out of all the samples taken, the concentrations reached their peak at the 5 inch ports 14 hours and 48 minutes after injection, with a dramatic decline at the following ports and sampling times. However, these results suggest that the dye was able to estimate the arrival of the bacteria. At the 5 inch ports, the *E. coli* cells reached the ports at 13 hours and 42 minutes, and by the next sampling time increased. At the 15 inch ports, the *E. coli* cells

reached the ports at 40 hours and 30 minutes, and decreased in concentration by the next sampling time. This trend was paralleled at the 25 and 35 inch ports, eventually going to 0 CFU/mL by the outlet. The *E. coli* was either not able to reach the outlet or died before sampling was completed. The rate of travel through the tank might vary depending on the initial packing. There might also be the presence of preferential flow which could cause the differences in concentration between the ports. While this experiment suggested that the visual tracer could be used to estimate the arrival of the bacteria, complete bacterial breakthrough curves could not be created, so the actual peak concentration could not be considered conclusive. Since the dye was used as a visual tracer and concentrations were not collected, a general statement cannot be made of the exact accuracy of the dye in predicting the arrival of the indicators.

Flushing of tank. After the second experiment, *E. coli* was injected into the reservoir. Background samples taken in the tank detected no *E. coli* cells, and a sample from the reservoir showed that the initial concentration was about $2 \times 10^5\ CFU/mL$. However, subsequent samplings from the tank detected no *E. coli* cells at any port. As described in the Materials and Methods Section, flushing up until this point had been done at the same flowrate as the model studies in the tank, which would take 2-3 weeks to wash once with chlorine and twice with tap water before resuming the *E. coli* experiments. After the attempt when *E. coli* was detected in the reservoir but not in the tank, flushing was done at very high flowrates to encourage the removal of any formed biofilms which might have accumulated and could be preventing the transport of the injected *E. coli*. This flushing brought a lot of material to the surface of the tank and was

subsequently discharged, including rust, discolored fluids, and even some residual dye, even though the dye tracer test at that point had been completed almost 3 months prior. Flushing at high rate could be done 3-4 times in a matter of hours.

***E. coli* Breakthrough, Exp. 3: Pressure Flow.** After determining that the results from the dye tracer test could be used as a rough model for the sampling of the bacteria, and flushing was done to remove any existing blockage, *E. coli* was injected again into the tank with an initial reservoir concentration of approximately $1.5 \times 10^5\ CFU/mL$, and bacterial breakthrough graphs were created for each sampling port based off of the sampling schedule shown previously in Table 4.2. Samples were taken multiple times at each port. However, prior to this experiment, a few hours had elapsed where water in the reservoir ran out and air was injected into the tank. The trapped air inside the tank prevented sampling at a few ports throughout the tank, including the 5L port, so data could not be obtained for this port. Figures 4.11, 4.12, and 4.13 summarize the bacterial breakthrough curves for the 5 inch, 15 inch, and 25 inch ports, respectively. No *E. coli* cells were detected at the 35 inch port.

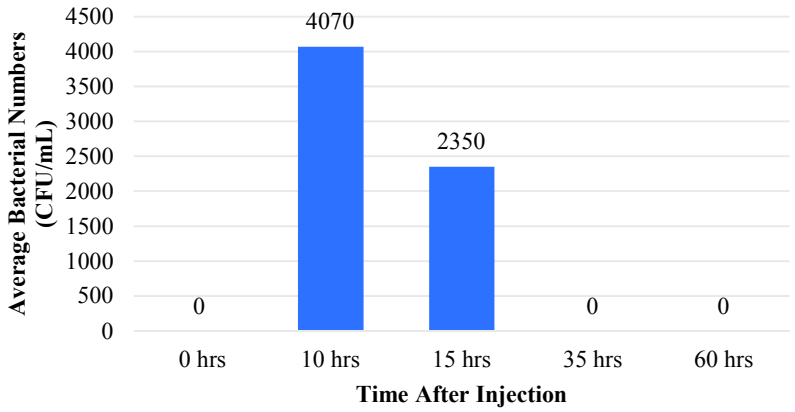

Figure 4.11 Transport of *E. coli* Over Time, Pressure Flow, 5 inch

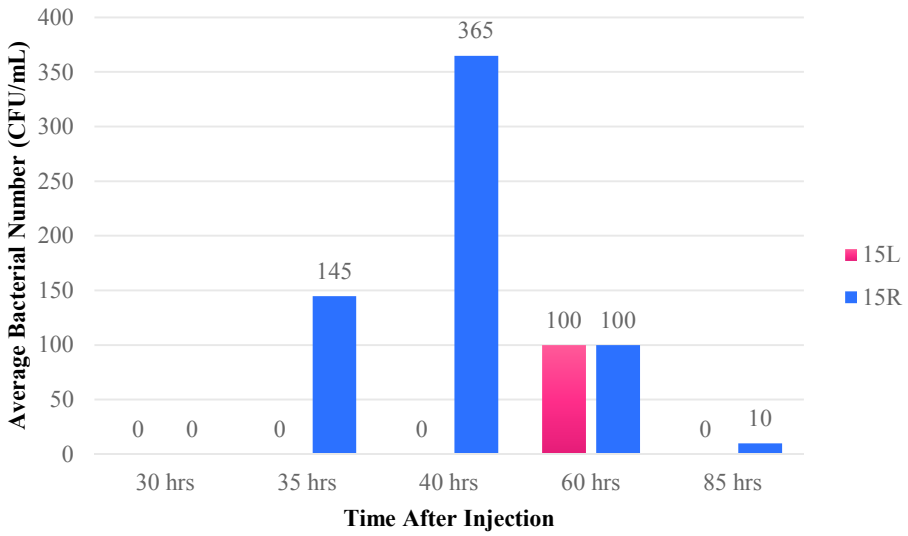

Figure 4.12 Transport of *E. coli* Over Time, Pressure Flow, 15 inch

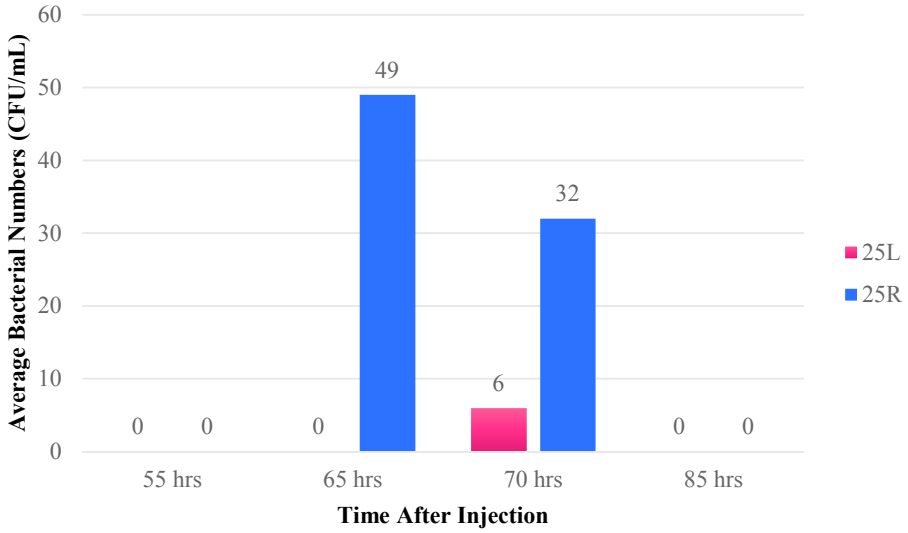

Figure 4.13 Transport of *E. coli* Over Time, Pressure Flow, 25 inch

Background concentrations before the start of the experiment showed that there was no *E. coli* detected in the tank. The concentration of *E. coli* in the tank after injection was consistently higher in the samples eluted from the right side sampling ports. Out of

all the samples taken, the concentrations reached their peak at the 5 inch ports 10 hours after injection, with a dramatic decline at the following ports and sampling times. The 5 inch port breakthroughs seem to be earlier than those predicted by the tracer, which was around 14 hours. This could be due to mechanical mixing and dispersion within the soil, which would account for why the arrival of the microbial indicator was so much earlier than expected, as explained in the Literature Review. Apart from the 5 inch, the breakthrough concentration arrival times were closer to those predicted by the tracer. The *E. coli* was either not able to reach the 35 inch ports or died before sampling was completed.

Overall, concentrations for this experiment were considerably lower than the previous experiments, despite the high rate flushing and attempt to remove blockage. Though there was qualitative agreement between the behavior of the *E. coli* throughout the experiments, quantitative agreement could not be made and there was difficulty in reproducing similar results. These results may suggest that pressure flow does not yield sufficient representation of the transport of the bacteria, and that gravity flow should be attempted, which could be considered more similar to conditions which would occur in the field in the case of leeching from the surface into soils.

Transport of E. coli, Exp. 4: Gravity Flow. After determining that pressure flow results could not be reproduced and quantitative agreement could not be obtained, the set up of the tank was changed (Figure 3.11) so that transport with gravity flow could be investigated. Prior to this experiment, the tank was drained and left unsaturated for 24 hours. The tank was filled again from the bottom to prevent any trapped air, disinfected

with chlorine, and washed through 2 more times with tap water. *E. coli* was injected again into the tank with an initial reservoir concentration of approximately $1.1 \times 10^5\ CFU/mL$, and bacterial breakthrough graphs were created for each sampling port based off of the sampling schedule shown previously in Table 4.2. Samples were taken multiple times at each port. Figures 4.14 through 4.17 summarize the results.

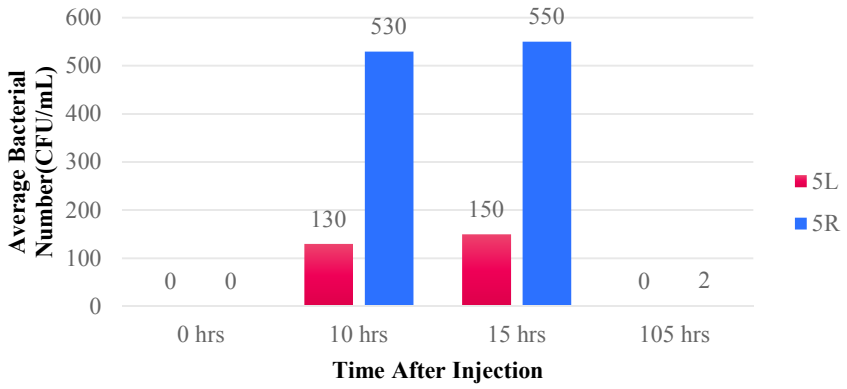

Figure 4.14 Transport of *E. coli* Over Time, Gravity Flow, 5 inch

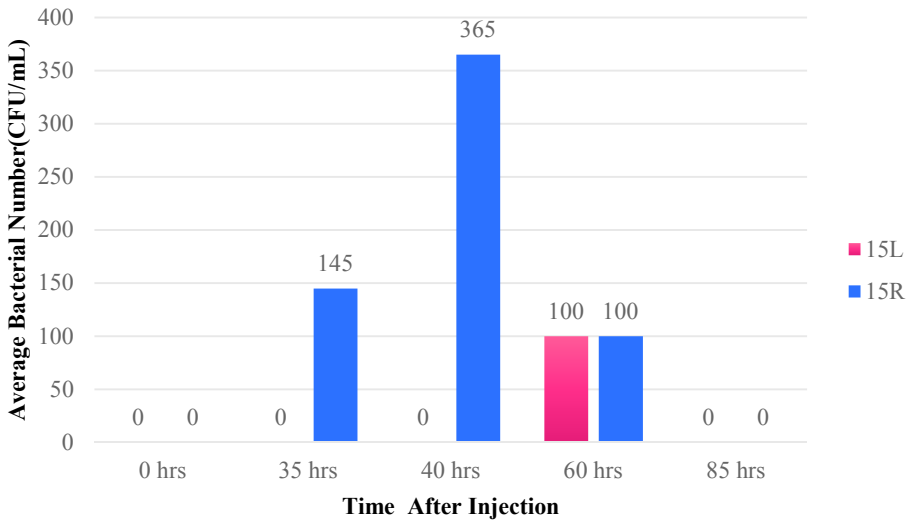

Figure 4.15 Transport of *E. coli* Over Time, Gravity Flow, 15 inch

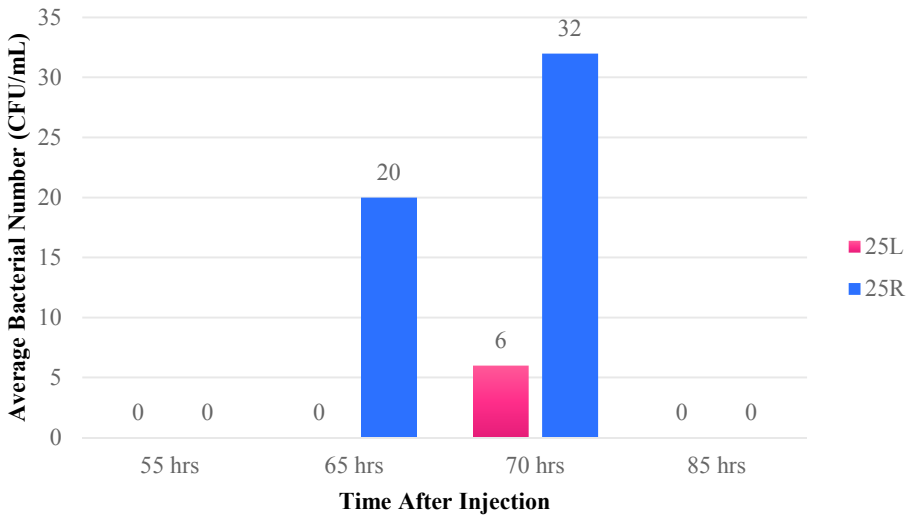

Figure 4.16 Transport of *E. coli* Over Time, Gravity Flow, 25 inch

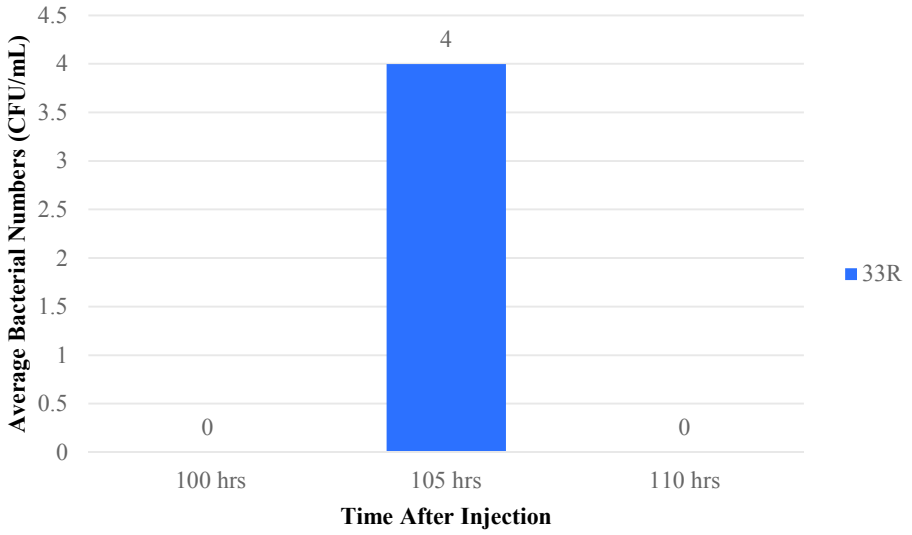

Figure 4.17 Transport of *E. coli* Over Time, Gravity Flow, 33 inch

Background concentrations before the start of the experiment showed that there was no *E. coli* detected in the tank. The concentration of *E. coli* in the tank after injection was consistently higher in the samples eluted from the right side sampling ports. Out of all the samples taken, the concentrations reached their peak at the 5 inch ports 15 hours after injection. Like pressure flow, the 5 inch port breakthroughs seem to be earlier than those predicted by the tracer, which was around 14 hours. Apart from the 5 inch port, the breakthrough concentration arrival times were closer to those predicted by the tracer. Since the "orientation" of the tank had been switched to gravity flow, there was no longer a sampling port available 35 inches from the inlet, so instead sampling was done at the 33 inch port. With gravity flow, *E. coli* cells were able to be detected at the 33 inch port. This may be attributed to gravity flow, or that it was 33 inches from the inlet and not 35 inches, so the *E. coli* cells had to travel less distance.

Transport of *E. coli*, Exp. 6: Gravity Flow. *E. coli* was injected into the reservoir to obtain an initial concentration of approximately $2.4 \times 10^5\ CFU/mL$, and bacterial breakthrough graphs were created for the sampling ports based off of the sampling schedule shown previously in Table 4.2. Samples were taken multiple times at each port. However, the experiment was discontinued after obtaining results from the assay from 15 hours after injection. The concentrations were extremely low at the 5 inch ports, and no cell were detected from the samples collected from the 15 inch ports, despite high rate flushing and gravity flow. Figure 4.18 shows the data that was collected for this experiment.

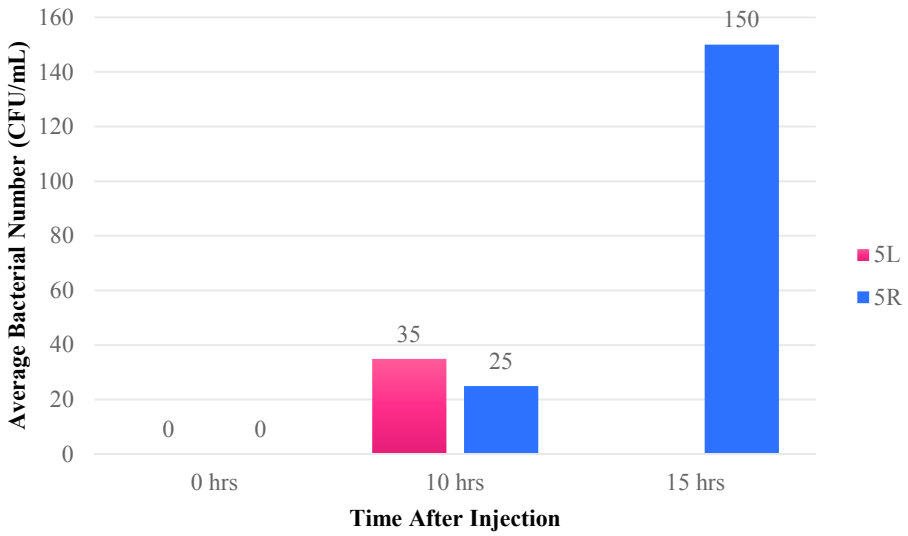

Figure 4.18 Transport of *E. coli* Over Time, Gravity Flow, 5 inch

Background concentrations before the start of the experiment showed that there was no *E. coli* detected in the tank. 10 hours after injection, for the first time in any experiment, the concentration was higher on the left side than on the right, even though no cells were detected on the left side after 15 hours, and 150 CFU/mL was found at the same time on the right side

Spiked Dose P22 Experiments, Gravity Flow

Transport of P22 over time, Exp. 1. The stability of P22 phage was investigated, the results of which can be found in Table 3.3 in the Materials and Methods Section. P22 was determined to be relatively stable, though it did experience die-off. For all P22 experiments, the concentration in the reservoir was tracked over time along with the concentrations at the sampling ports. Reservoir stability and bacterial breakthrough graphs were created and can be seen summarized in Figures 4.19 through 4.22. The 33R

sampling port was only sampled once with a concentration of 550 PFU/mL 85 hours after injection. These graphs can be prepared with the predicted arrival times summarized in Table 4.3. For all experiments, background concentrations were taken before commencing to ensure there was no P22 detected in the tank.

Table 4.3 Summary of Predicted Arrival Times at Each Port

Sampling Port	Predicted Arrival Times (hr:min)	
	Left	Right
5 in	14:48	13:42
15 in	42:12	40:30
25 in	69:36	67:18
33 in	91:30	88:48

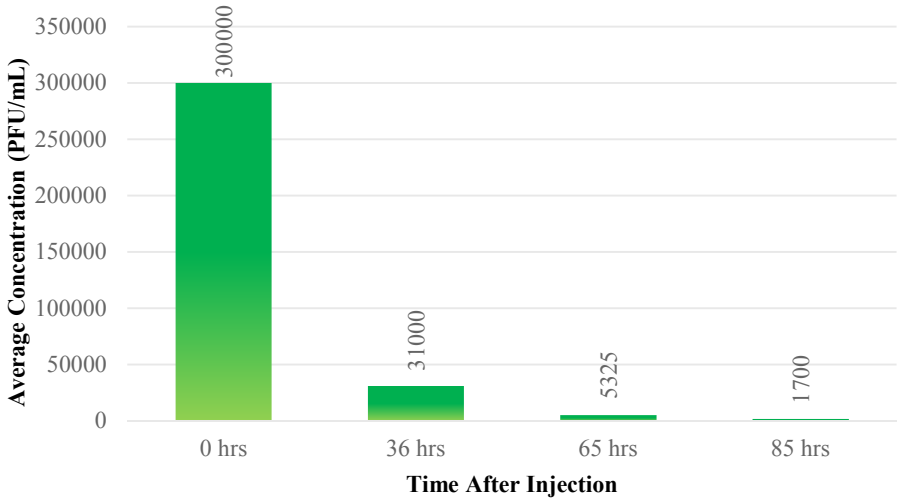

Figure 4.19 Reservoir Stability

Though the reservoir did experience die-off or inactivation, the log reduction after 36 hours was around 1 log, as compared to 3 log reduction after 24 hours that *E. coli* experienced. After 85 hours, P22 was still detected in the reservoir with after experiencing 2 log reduction total from the start of the experiment.

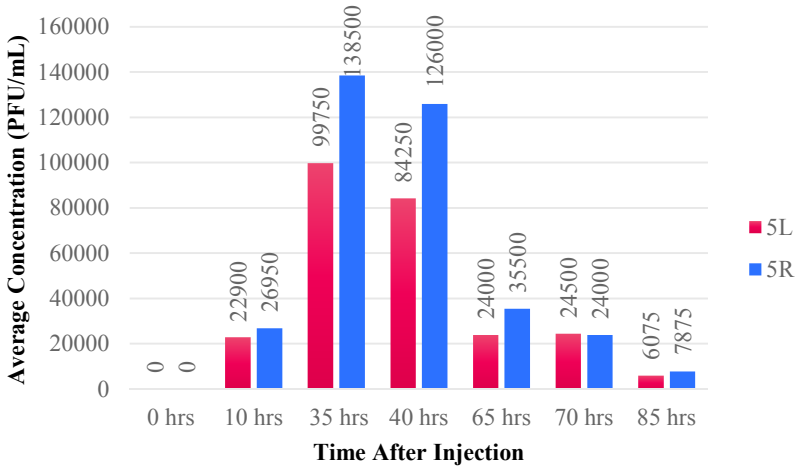

Figure 4.20 Transport of P22 Over Time, Gravity Flow, 5 inch

P22 was detected at the 10 hour sampling and out of all the samples taken, reached its peak 35 hours after injection that was similar to the initial reservoir concentration. Concentrations declined gradually after this peak and P22 was still detected after 85 hours after an approximate 2 log reduction total.

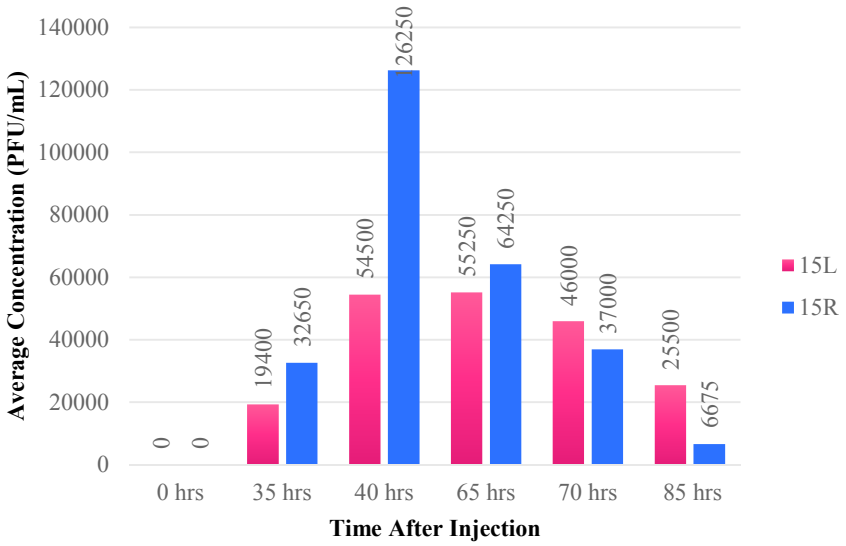

Figure 4.21 Transport of P22 Over Time, Gravity Flow, 15 inch

P22 was detected at the 35 hour sampling and out of all the samples taken, reached its peak 40 hours after injection that was similar to the initial reservoir concentration. Concentrations declined gradually after this peak and P22 was still detected after 85 hours after an approximate 2 log reduction total.

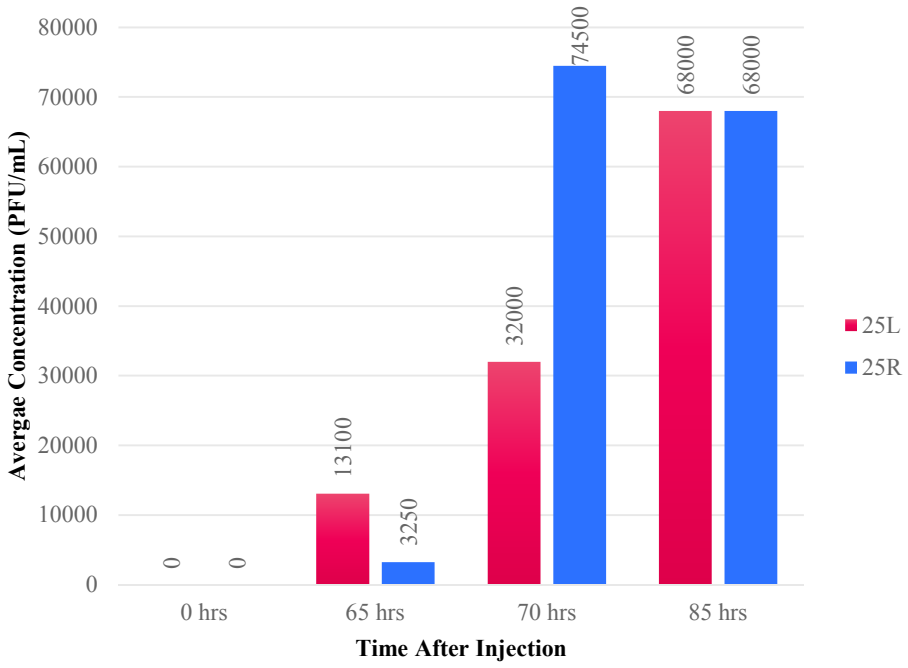

Figure 4.22 Transport of P22 Over Time, Gravity Flow, 25 inch

P22 was detected at the 65 hour sampling and out of all the samples taken, reached its peak 70 hours after injection that was similar to the initial reservoir concentration. Concentrations declined slightly after this peak and P22 was still detected after 85 hours after approximately 1 log reduction total.

A summary of the results at all ports can be seen in Figures 4.23 and 4.24.

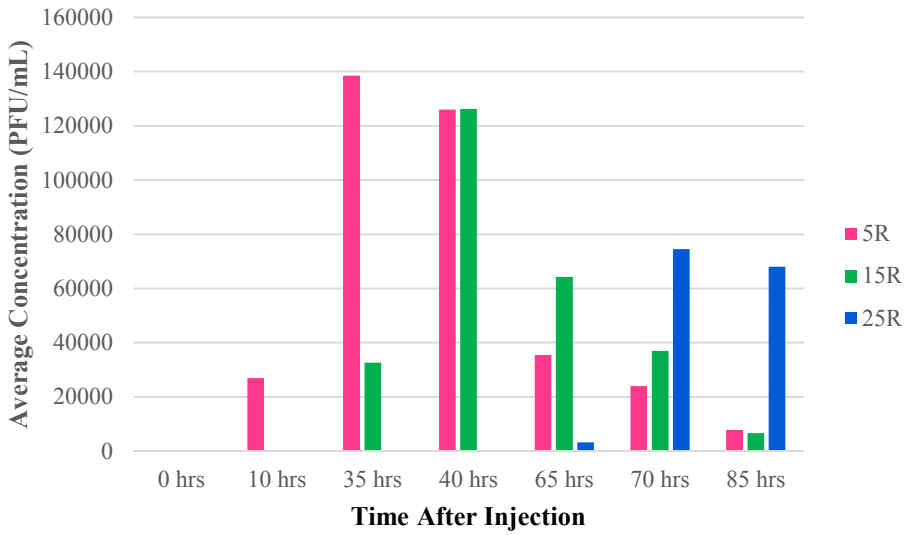

Figure 4.23 Summary of transport of P22 over time, right side ports

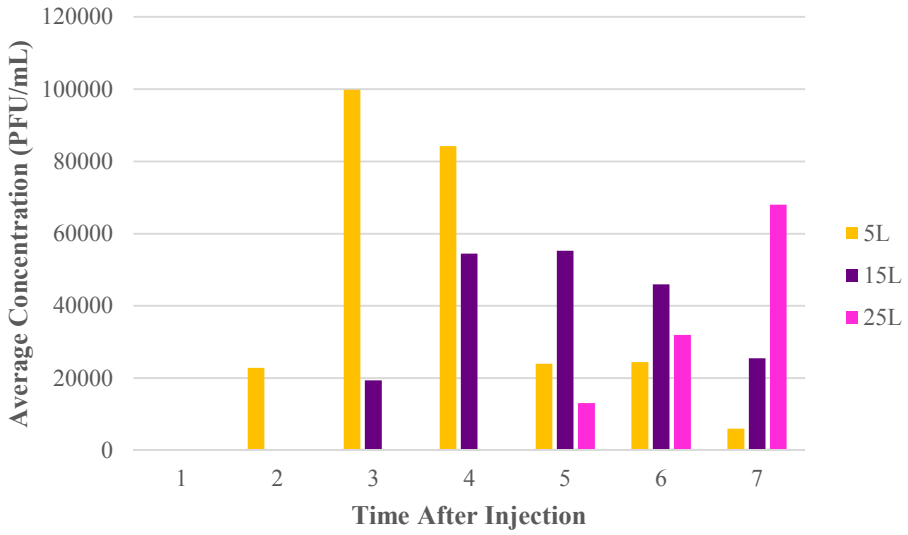

Figure 4.24 Summary of Transport of P22 Over Time, Left Side Ports

With a few exceptions, the concentrations eluted from the right side ports were still consistently higher than from the left side. The peak concentrations for each sampling port were similar to the initial reservoir concentration, with a gradual decline following the peak, and breakthrough was reached at a time close to those predicted by the tracer. The results are comparable to those found in other lab studies; the saturated flow conditions allowed for little to no adsorption of the phage to the soil, rapid transport and survival greater than 72 hours. Considered in conjunction with the results from the *E. coli* experiments, these results support the claim that bacteriophages move through soil easier and with greater recovery than bacteria.

Transport of P22 over time, Exp. 2. Reservoir stability and bacterial breakthrough graphs were created and can be seen summarized in Figures 4.25 through 4.28. Sampling ports 33R and 33L were sampled once, obtaining concentrations of 300 PFU/mL and 200 PFU/mL, respectively, 85 hours after injection. The results of the second experiment were similar to those from the first experiment; though the concentrations were all slightly lower in the second experiment, the trends were all the same.

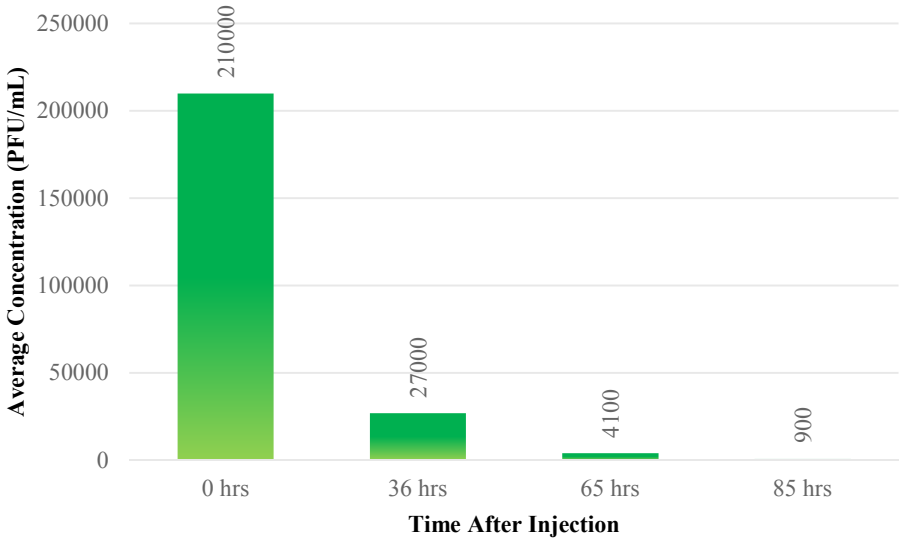

Figure 4.25 Reservoir Stability

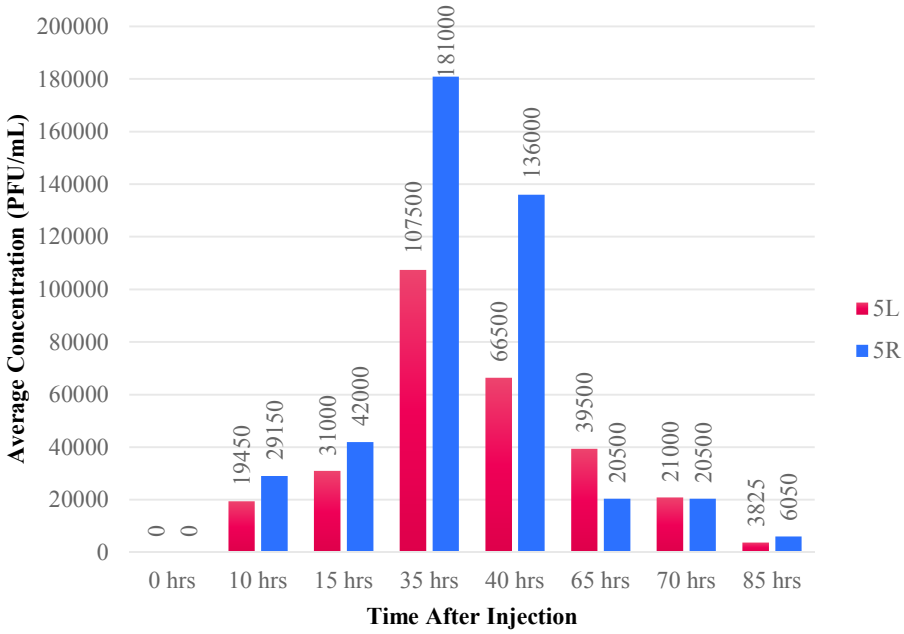

Figure 4.26 Transport of P22 Over Time, Gravity Flow, 5 inch

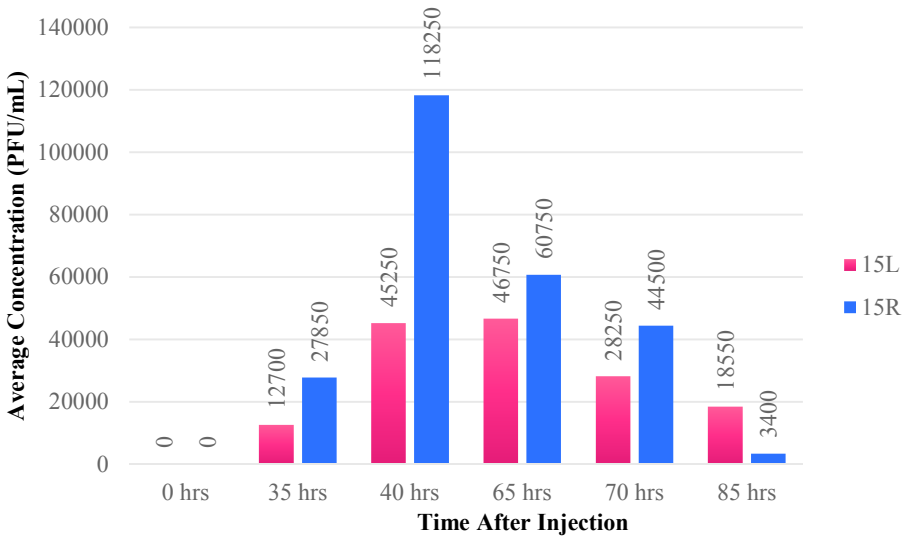

Figure 4.27 Transport of P22 Over Time, Gravity Flow, 15 inch

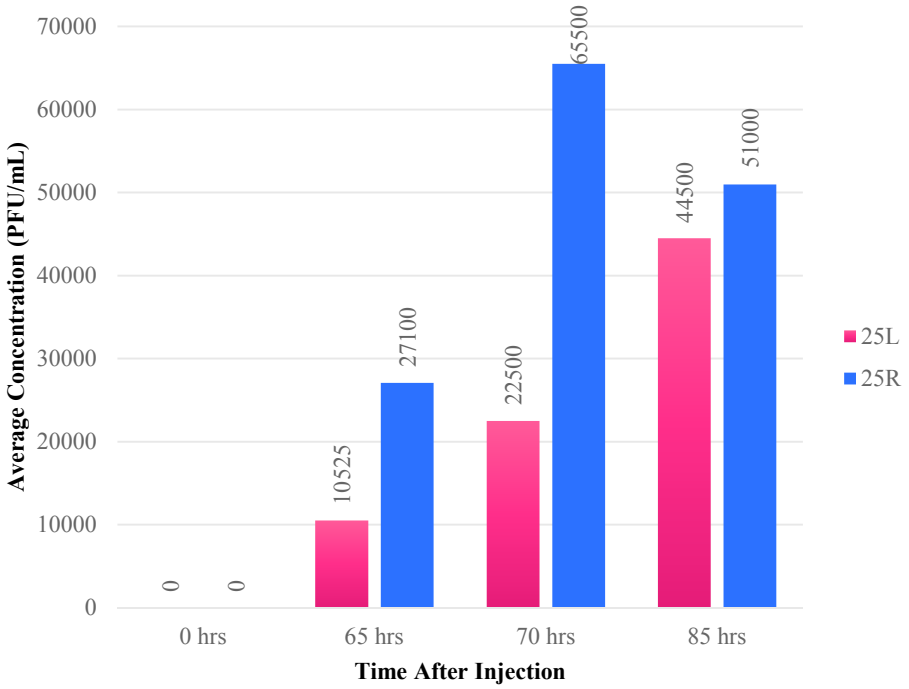

Figure 4.28 Transport of P22 Over Time, Gravity Flow, 25 inch

A summary of the results at all ports can be seen in Figures 4.29 and 4.30.

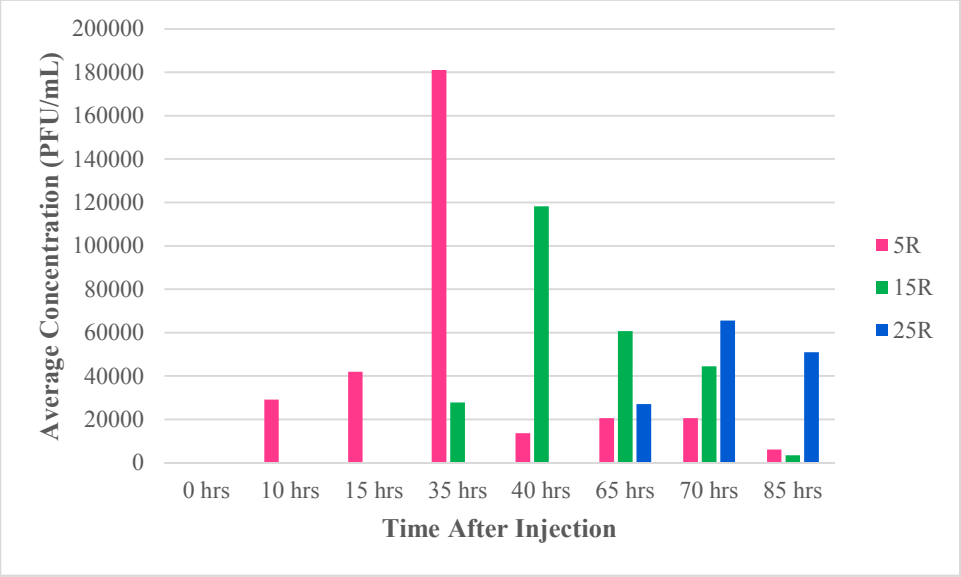

Figure 4.29 Summary of Transport of P22 Over Time, Right Side Ports

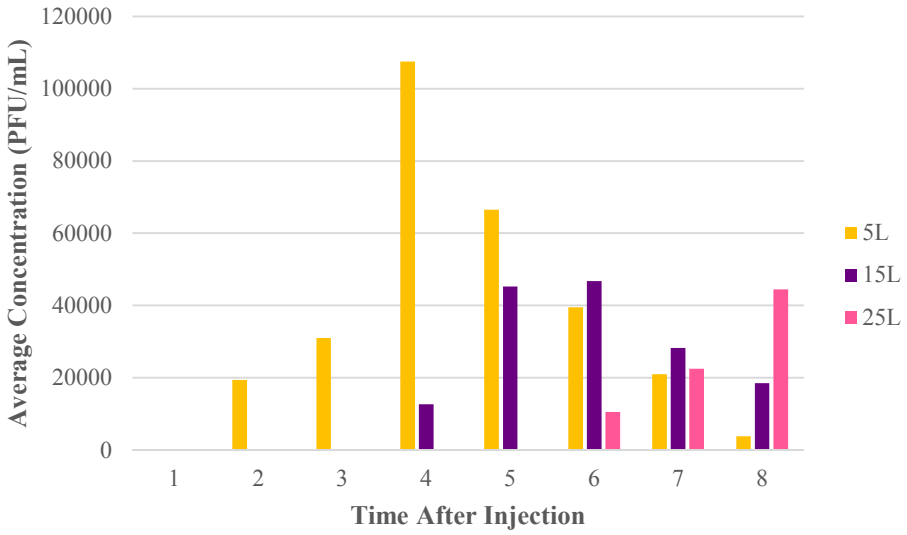

Figure 4.30 Summary of Transport of P22 Over Time, Left Side Ports

Transport of P22 over time, Exp. 3. The third experiment with P22 did not go as expected and did not produce similar results with the last two experiments, even though none of the procedures or parameters were changed. The initial concentration was found

to be 56,500 PFU/mL, and after 35 hours no P22 was able to be detected in the reservoir. Bacterial breakthrough graphs were created for the sampling ports and can be seen summarized in Figures 4.31 through 4.33. Sampling ports 33R and 33L were sampled once, obtaining concentrations of 150 PFU/mL and 0 PFU/mL, respectively, 85 hours after injection. It is not certain what might have occurred which made this experiment's results so much different from those previous. The procedures were not altered and yet the concentrations were considerably smaller, the left side concentrations were higher than the right side, and after 85 hours P22 was no longer detected at the 5 inch ports, and was not detected at the 33L port.

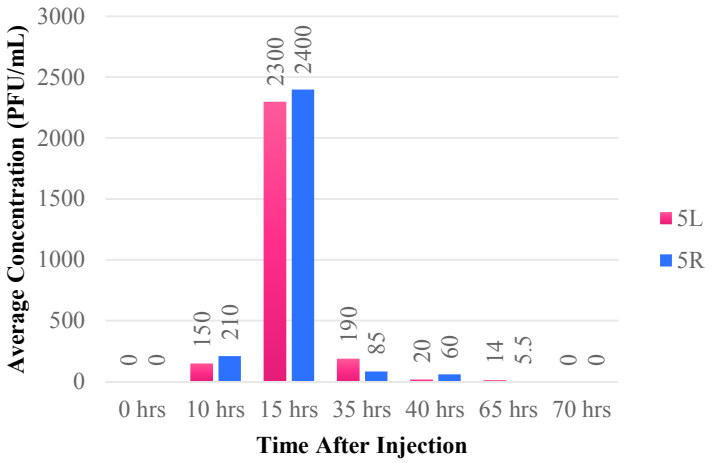

Figure 4.31 Transport of P22 Over Time, Gravity Flow, 5 inch

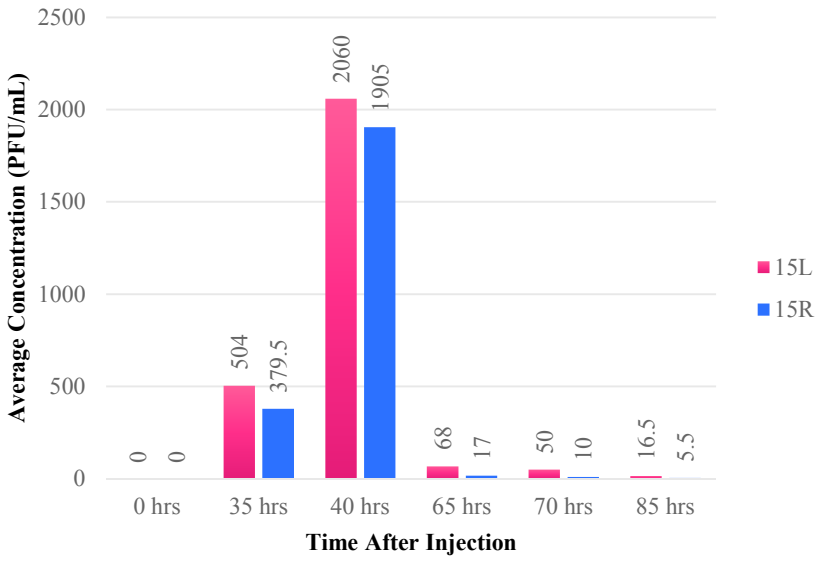

Figure 4.32 Transport of P22 Over Time, Gravity Flow, 15 inch

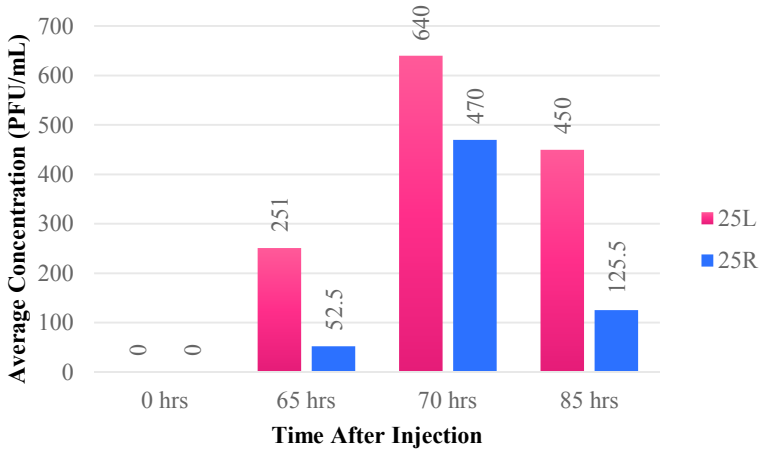

Figure 4.33 Transport of P22 Over Time, Gravity Flow, 25 inch

A summary of the results at all ports can be seen in Figures 4.34 and 4.35.

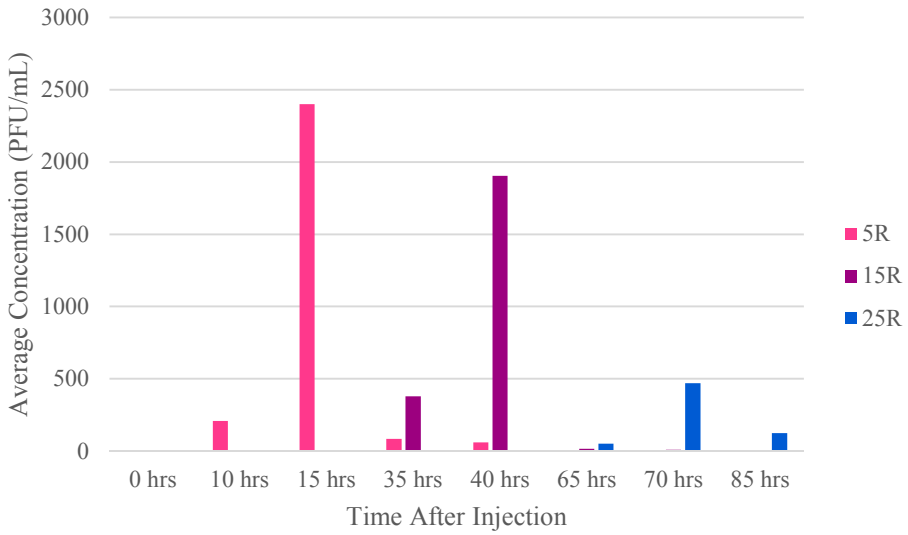

Figure 4.34 Summary of Transport of P22 Over Time, Right Side Ports

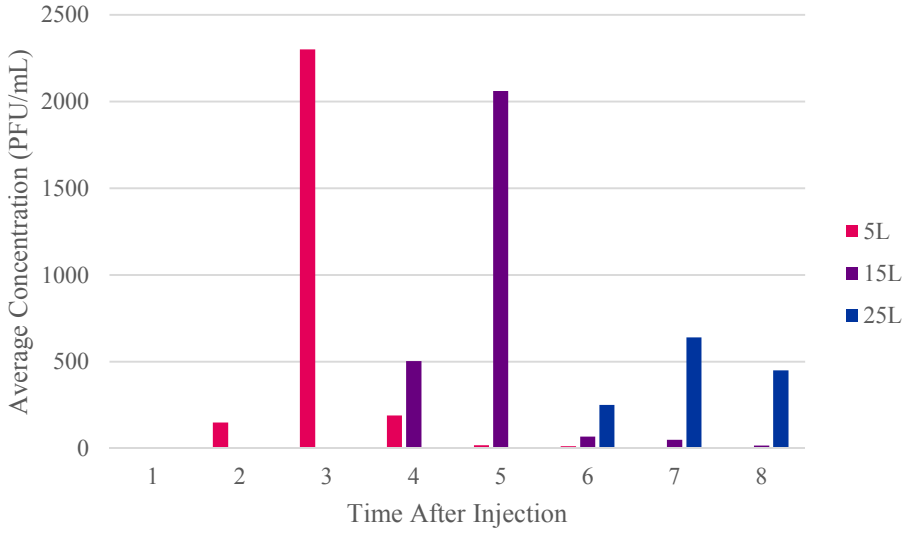

Figure 4.35 Summary of Transport of P22 Over Time, Left Side Ports

A final summary of the P22 experiments can be compiled and seen in Figures 4.36 and 4.37. The values are the average of the first two experiments with two replicates.

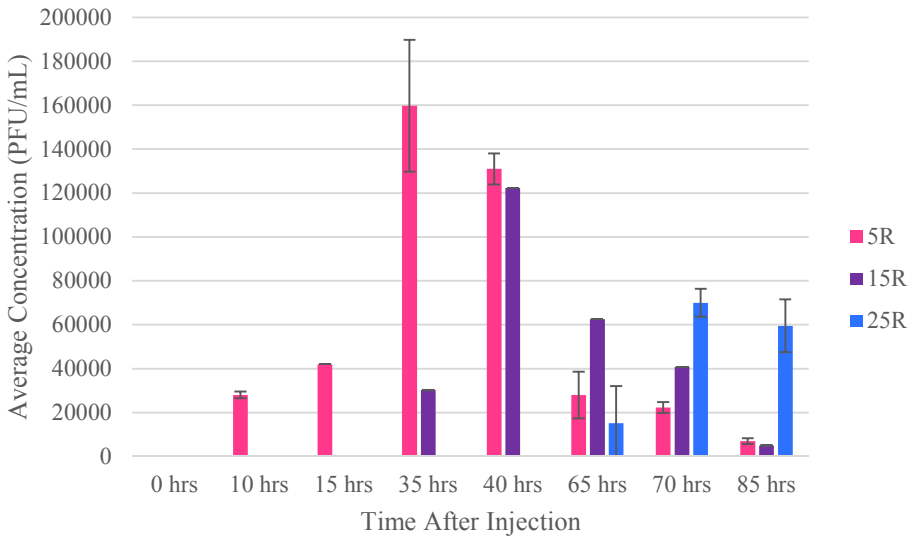

Figure 4.36 Transport of P22 Over Time, Right Side Ports

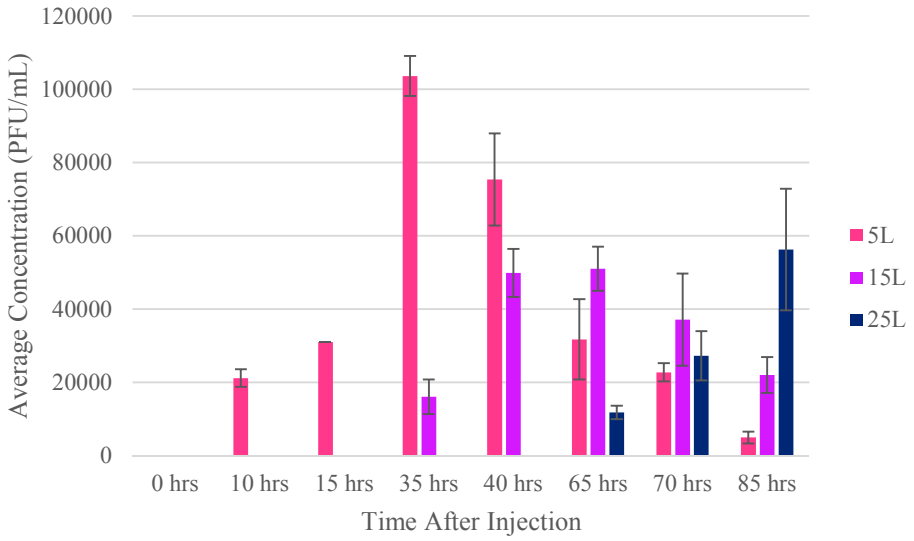

Figure 4.37 Transport of P22 Over Time, Left Side Ports

CONCLUSION

The purpose of this study was to investigate and document the transport of bacterial and viral indicators through a 2 dimensional packed porous media model, and the objectives set forth were met. *E. coli* and P22 were the bacteria and bacteriophage selected for the study, respectively, and were transported through a packed tank. Fluid phase concentrations were collected from sampling ports at intermittent times after injection based off of a sampling schedule established from estimations from a dye tracer test. The dye travel rate was found to be 0.36 in/hr for the left side of the tank and 0.37 in/hr for the right side. For the vast majority of the results for *E. coli* and P22, the concentrations eluted from the right side of the tank were consistently higher than those from the left side of the tank. There are several limitations that are inherent with the estimations of the arrival of the dye at the sampling ports, and since the dye was used as a visual tracer and fluid-phase concentrations were not measured, a general statement cannot be made of the exact accuracy of the dye in predicting the arrival of the bacteria. Instead, the visual tracer was used to construct a rough estimation of when sampling for the microbial indicators could be completed. The rate of travel of bacteria through the tank might vary depending on the initial packing. There might be the presence of preferential flow, which could cause the differences in concentration between the ports. Mechanical mixing and dispersion within the soil could also account for why the arrival of the microbial indicators at the ports was earlier than expected.

The results suggest that pressure flow does not yield sufficient representation of the transport of *E. coli*, possibly demonstrated by the lack of reproducibility of results

under pressure flow conditions, and no recovery of the bacteria in the effluent. Gravity flow allowed for *E. coli* to be transported to the farthest available sampling port from the inlet, which may be attributed to gravity flow. Overall, the similarity of this study to the one conducted by Bradford et al. suggest that the decreasing and low recovery of *E. coli* over time is most likely due to straining and physical filtration as described in the literature review. *E. coli* was either filtered out and prevented from travelling long distances and was not able to reach the outlet, or inactivated before the sampling was completed. After breakthrough, *E. coli* concentrations quickly reached their peak, with a dramatic decline at the following ports and sampling times. Though there was qualitative agreement between the behavior of *E. coli* throughout the experiments, quantitative agreement could not be made and there was difficulty in reproducing similar results.

P22 was determined to be stable in the reservoir, though it did experience die-off. For all P22 experiments, the concentration in the reservoir was tracked over time along with the concentrations at the sampling ports. The bacteriophage experienced approximately 1 log reduction after 36 hours in the reservoir. After 85 hours, P22 was still detected in the reservoir with after experiencing 2 log reduction total from the start of the experiment. The peak concentrations for each sampling port were similar to the initial reservoir concentration, with a gradual decline following the peak, and breakthrough was reached at a time close to those predicted by the tracer. The results are comparable to those found in other studies; the saturated flow conditions might have allowed for little to no adsorption of the phage to the soil, resulting in rapid transport and survival greater than 72 hours. Juxtaposed with the results from *E. coli* experiments, these results support

the claim that bacteriophages move through soil faster and with greater recovery than bacteria.

Though some mean behavior and qualitative agreement was observed in the model studies in the selected media, and some results were similar to those of some column investigations, the limitations of this study make it premature to make definitive conclusions on field-scale behavior solely based on the results. However, the trends observed in the study can provide some insight into certain aspects of microbial transport in controlled systems, which could possibly be transferred to other, more complex systems. There are myriad factors which influence transport in real-world situations and applications and must be considered. However, since microbial transport was documented in this study, it can be concluded that the mechanism of pathogen transport exists under recharge practices.

Further Investigations

Further studies are needed with varying transport factors to improve overall understanding of microbial transport kinetics. Some goals for future studies could include establishing a level of reproducibility of the results in conducting more experiments. Also, since it is presumed that filtration prevented the detection of *E. coli* at later times and farther distances from the outlet, fluid phase concentrations could be paired with a distribution of solids as a function of distance to demonstrate spatial variability. If completed, the amount of deposition and attachment of *E. coli* cells to the surfaces of the sand grains could be estimated. Another limitation of the study was that the sampling process methods could only detect live cells eluted from the sampling ports; further

investigations could explore inactivation by measuring concentrations of both live and dead cells from the model. Other studies could investigate the fate and transport of other bacteria, such as *Legionella,* to provide more comprehensive knowledge of pathogenic bacterial transport.

REFERENCES

Abbaszadegan, M., Mayer, B. K., Ryu, H., & Nwachuku, N. (2007). Efficacy of Removal of CCL Viruses under Enhanced Coagulation Conditions. *Environmental Science & Technology,41*(3), 971-977. doi:10.1021/es061517z

Abbaszaedgan, M., Rauch-Williams, T., Johnson, W. P., & Hubbs, S. A. (2011). Methods to Assess GWUDI and Bank Filtration Performance. *Water Research Foundation.*

Abu-Abshour, J., Joy, D. M., Lee, H., Whiteley, H. R., & Selin, S. (1994). Transport of microorganisms through soil. *Water, Air, and Soil Pollution, 75*(1-2), 141-158. doi:10.1007/bf01100406

Ahn, J., & Biswas, D. (2014). Influence of bacteriophage P22 on the inflammatory mediator gene expression in chicken macrophage HD11 cells infected with *Salmonella* Typhimurium. *FEMS Microbiology Letters,352*(1), 11-17. doi:10.1111/1574-6968.12379

American Society for Microbiology. (n.d.). Retrieved 2017, from https://www.asm.org/division/m/M.html

Barak, J. D., & Liang, A. S. (2008). Role of Soil, Crop Debris, and a Plant Pathogen in *Salmonella enterica* Contamination of Tomato Plants. *PLoS ONE,3*(2). doi:10.1371/journal.pone.0001657

Bradford, S. A., Simunek, J., & Walker, S. L. (2006). Transport and straining of E. coli O157:H7 in saturated porous media. *Water Resources Research,42*(12). doi:10.1029/2005wr004805

Casjens, S. (2000). Information about bacteriophage P22- American Society for Microbiology . Retrieved 2017, from https://www.asm.org/division/m/fax/P22Fax.html

Casjens, S., & Lenk, E. (2000, August 15). Electron micrograph of bacteriophage P22. Retrieved 2017, from https://www.asm.org/division/m/foto/P22Mic.html

Centers for Disease Control and Prevention. (2015, November 06). Retrieved 2017, from https://www.cdc.gov/ecoli/general/index.html

Centers for Disease Control and Prevention. (2017, June 01). Retrieved https://www.cdc.gov/*salmonella*/index.html

Commercial Grade Sands: Product Nos. 1961, 1962, 1963 [Pamphlet]. (n.d.). Atlanta, GA: the QUIKRETE Companies©.

Corapcioglu, M.Y., & Haridas, A. (1984). Transport and fate of microorganisms in porous mdia: A theoretical investigation. *Journal of Hydrology, 72*(1-2), 149-169. doi:10.1016/0022-1694(84)90189-6

Debordea, D. C., Woessnerb, W. W., Kileyb, Q. T., & Balla, P. (1999). Rapid transport of viruses in a floodplain aquifer. *Water Research,33*(10), 2229-2238. doi:10.1016/s0043-1354(98)00450-3

ESCHERICHIA COLI - PATHOGEN SAFETY DATA SHEET - INFECTIOUS SUBSTANCES. (2012, April 30). Retrieved 2017, from http://www.phac-aspc.gc.ca/lab-bio/res/psds-ftss/escherichia-coli-pa-eng.php

Grit Sizes – ANSI. (2017). Retrieved 2017, from http://www.washingtonmills.com/guides/grit-sizes-ansi/particle-size-conversion-chart-ansi/

Gupta, V., Johnson, W. P., Shafieian, P., Ryu, H., Alum, A., Abbaszedegan, M., Hubbs, S. A., Rauch-Williams, T. (2009). Riverband Filtration: Comparison of Pilot Scale Transport with Theory. *Environmental Science & Technology, 43*(3), 669-676. doi:10.1021/s8016396

Hardy Diagnostics. (2016). Retrieved 2017, from https://catalog.hardydiagnostics.com/cp_prod/Content/hugo/*Salmonella*.htm

Hartford University. (2001, November). Retrieved 2017, from http://uhavax.hartford.edu/bugl/microbe.htm

Ingham, S. C., Losinski, J. A., Andrews, M. P., Breuer, J. E., Breuer, J. R., Wood, T. M., & Wright, T. H. (2004). *Escherichia coli* Contamination of Vegetables Grown in Soils Fertilized with Noncomposted Bovine Manure: Garden-Scale Studies. *Applied and Environmental Microbiology,70*(11), 6420-6427. doi:10.1128/aem.70.11.6420-6427.2004

Ishii, S., Ksoll, W. B., Hicks, R. E., & Sadowsky, M. J. (2006). Presence and Growth of Naturalized *Escherichia coli* in Temperate Soils from Lake Superior Watersheds. *Applied and Environmental Microbiology,72*(1), 612-621. doi:10.1128/aem.72.1.612-621.2006

Minogue, T. D., Daligault, H. A., Davenport, K. W., Bishop-Lilly, K. A., Broomall, S. M., Bruce, D. C., . . . Johnson, S. L. (2014). Complete Genome Assembly of Escherichia coli ATCC 25922, a Serotype O6 Reference Strain. *Genome Announcements,2*(5). doi:10.1128/genomea.00969-14

P22 Bacteriophage (Molecular Biology). (n.d.). Retrieved 2017, from http://what-when-how.com/molecular-biology/p22-bacteriophage-molecular-biology/

Park, J., Kang, J., & Kim, S. (2017). Comparative Analysis of Bacteriophages and Bacteria Removal in Soils and Pyrophyllite-Amended Soils: Column Experiments. *Water, Air, & Soil Pollution,228*(3). doi:10.1007/s11270-017-3288-6

Powelson, D. K., Simpson, J. R., & Gerba, C. P. (1990). Virus Transport and Survival in Saturated and Unsaturated Flow through Soil Columns. *Journal of Environment Quality,19*(3), 396. doi:10.2134/jeq1990.00472425001900030008x

Sanders, C., & Brophy-Martinez, K. (2007, February). *Chapter 16 Clinical Microbiology: Enterobacteriaceae* [PPT]. Austin: Austin Community College District.

Shen, C., Phanikumar, M. S., Fong, T. T., Aslam, I., Mcelmurry, S. P., Molloy, S. L., & Rose, J. B. (2008). Evaluating Bacteriophage P22 as a Tracer in a Complex Surface Water System: The Grand River, Michigan. *Environmental Science & Technology,42*(7), 2426-2431. doi:10.1021/es702317t

Silliman, S. E., Dunlap, R., Fletcher, M., & Schneegurt, M. A. (2001). Bacterial transport in heterogeneous porous media: Observations from laboratory experiments. *Water Resources Research,37*(11), 2699-2707. doi:10.1029/2001wr000331

Slonczewski, J. L., & Foster, J. W. (2011). *Microbiology: An Evolving Science*(2nd ed.). Retrieved from http://www.wwnorton.com/college/biology/microbiology2/ch/10/etopics.aspx

Smith, M. S., Thomas, G. W., White, R. E., & Ritonga, D. (1985). Transport of Escherichia coli Through Intact and Disturbed Soil Columns1. *Journal of Environment Quality,14*(1), 87. doi:10.2134/jeq1985.00472425001400010017x

Tufenkji, N. (2007). Modeling microbial transport in porous media: Traditional approaches and recent developments. *Advances in Water Resources, 30*(6-7). 1455-1469. doi:10.1016/j.advwatres.2006.05.014

Washington State Department of Health . (n.d.). Retrieved 2017, from http://www.doh.wa.gov/CommunityandEnvironment/DrinkingWater/Contaminants/Coliform#TotalColi

World Health Organization. (2017). Retrieved 2017, from http://www.who.int/mediacentre/factsheets/fs125/en/

World Health Organization. (2017). Retrieved 2017, from http://www.who.int/mediacentre/factsheets/fs139/en/

Zinno, P., Devirgiliis, C., Ercolini, D., Ongeng, D., & Mauriello, G. (2014). Bacteriophage P22 to challenge *Salmonella* in foods. *International Journal of Food Microbiology,191*, 69-74. doi:10.1016/j.ijfoodmicro.2014.08.037

2016 City of Tempe Water Quality Report(pp. 5-7, Rep.). (2016). Tempe, AZ: City of Tempe.

APPENDIX A

COMMERICIAL GRADE QUIKRETE© DATA SHEET

COMMERCIAL GRADE SANDS

PRODUCT NOS. 1961, 1962, 1963

DIVISION **32**

Aggregate
32 15 00

PRODUCT DESCRIPTION

QUIKRETE® Commercial grade sands are narrowly graded clean dry silica sands. They are available in three grades, fine (No. 1961), medium (No. 1962) and coarse (No. 1963).

PRODUCT USE

QUIKRETE® Commercial grade sands are silica sands which can be used alone or in combinations to provide a variety of gradations for any commercial application requiring high quality silica sands.

SIZES

• Available in 50 lb (22.7 Kg) and 100 lb (45.4 Kg) bags.

TECHNICAL DATA

QUIKRETE® Commercial grade sand is available in the following sizes:

Grade	Predominant Size Range US sieve number (mm)
Coarse No. 1963	#12 - #30 (1.7-0.6 mm)
Medium No. 1962	#20 - #50 (0.8-0.3 mm)
Fine No. 1961	#30 - #70 (0.6-0.2 mm)

PRECAUTIONS

• NOT RECOMMENDED FOR ABRASIVE BLASTING

WARRANTY

The QUIKRETE® Companies warrant this product to be of merchantable quality when used or applied in accordance with the instructions herein. The product is not warranted as suitable for any purpose or use other than the general purpose for which it is intended. Liability under this warranty is limited to the replacement of its product (as purchased) found to be defective, or at the shipping companies' option, to refund the purchase price. In the event of a claim under this warranty, notice must be given to The QUIKRETE® Companies in writing. This limited warranty is issued and accepted in lieu of all other express warranties and expressly excludes liability for consequential damages.

The QUIKRETE® Companies
One Securities Centre
3490 Piedmont Rd., NE, Suite 1300, Atlanta, GA 30305
(404) 634-9100 • Fax: (404) 842-1425

** Refer to www.quikrete.com for the most current technical data, MSDS, and guide specifications*

www.quikrete.com

Commercial Grade Sands: Product Nos. 1961, 1962, 1963 [Pamphlet]. (n.d.). Atlanta, GA: the QUIKRETE Companies©.

APPENDIX B

ANSI PARTICLE SIZE CONVERSION CHART

Table 3.1 ANSI Particle Size Conversion Chart

Millimeters	Microns	Inches	ASTM	Tyler Sieve	*ANSI Table 2	*ANSI Table 3
5.60	5600	0.220	3 1/2	3 1/2	S-S	-
4.75	4750	0.187	4	4	4	-
4.00	4000	0.157	5	5	5	-
3.35	3350	0.132	6	6	6	-
2.80	2800	0.110	7	7	7	-
2.36	2360	0.093	8	8	8	-
2.00	2000	0.079	10	9	10	-
1.70	1700	0.067	12	10	12	-
1.40	1400	0.055	14	12	14	-
1.18	1180	0.046	16	14	16	16
1.00	1000	0.039	18	16	20	20
0.850	850	0.033	20	20	22	24
0.710	710	0.028	25	24	24	-
0.600	600	0.024	30	28	30	30
0.500	500	0.02	35	32	36	36
0.425	425	0.018	40	35	40	-
0.355	355	0.014	45	42	46	46
0.300	300	0.012	50	48	54	54
0.250	250	0.010	60	60	60	60
0.212	212	0.008	70	65	70	70
0.180	180	0.007	80	80	80	80
0.150	150	0.006	100	100	90	90
0.125	125	0.005	120	115	100	100
0.106	106	0.004	140	150	120	120
0.075	75	0.0030	200	200	150	150
0.063	63	0.0025	230	250	180	180
0.053	53	0.0021	270	270	220	220
0.045	45	0.0018	325	325	240	240

Micro Grits

Millimeters	Microns	Inches	ANSI Grit
0.0500	50.0	0.00200	240
0.0395	39.5	0.00156	280
0.0295	29.5	0.00116	320
0.0230	23.0	0.00091	360
0.0183	18.3	0.00072	400
0.0139	13.9	0.00055	500
0.0106	10.6	0.00042	600
0.0077	7.8	0.0003	800
0.0058	5.8	0.00023	1000
0.0038	3.8	0.00015	1200
0.0450	45	0.0018	F
0.0275	27.5	0.0011	FF
0.0160	16	0.00063	FFF
0.0110	11	0.00043	FFFF

*A grit size is defined by the distribution of grits retained on a sieve set up that meets the requirements of ANSI Table 2 or 3. The numbers in the two sieve columns in this chart represent the midpoint sieve for the grading of the corresponding grit size. We've chosen to show the midpoint sieve since more material will be retained on this sieve than on any other in the sieve set up.

*Columns Tyler Sieve, ANSI Table 2, and ANSI Table 3 correspond to grit size

Grit Sizes – ANSI. (2017). Retrieved 2017, from http://www.washingtonmills.com/guides/grit-sizes-ansi/particle-size-conversion-chart-ansi/

APPENDIX C

LABORATORY TANK PHOTOS

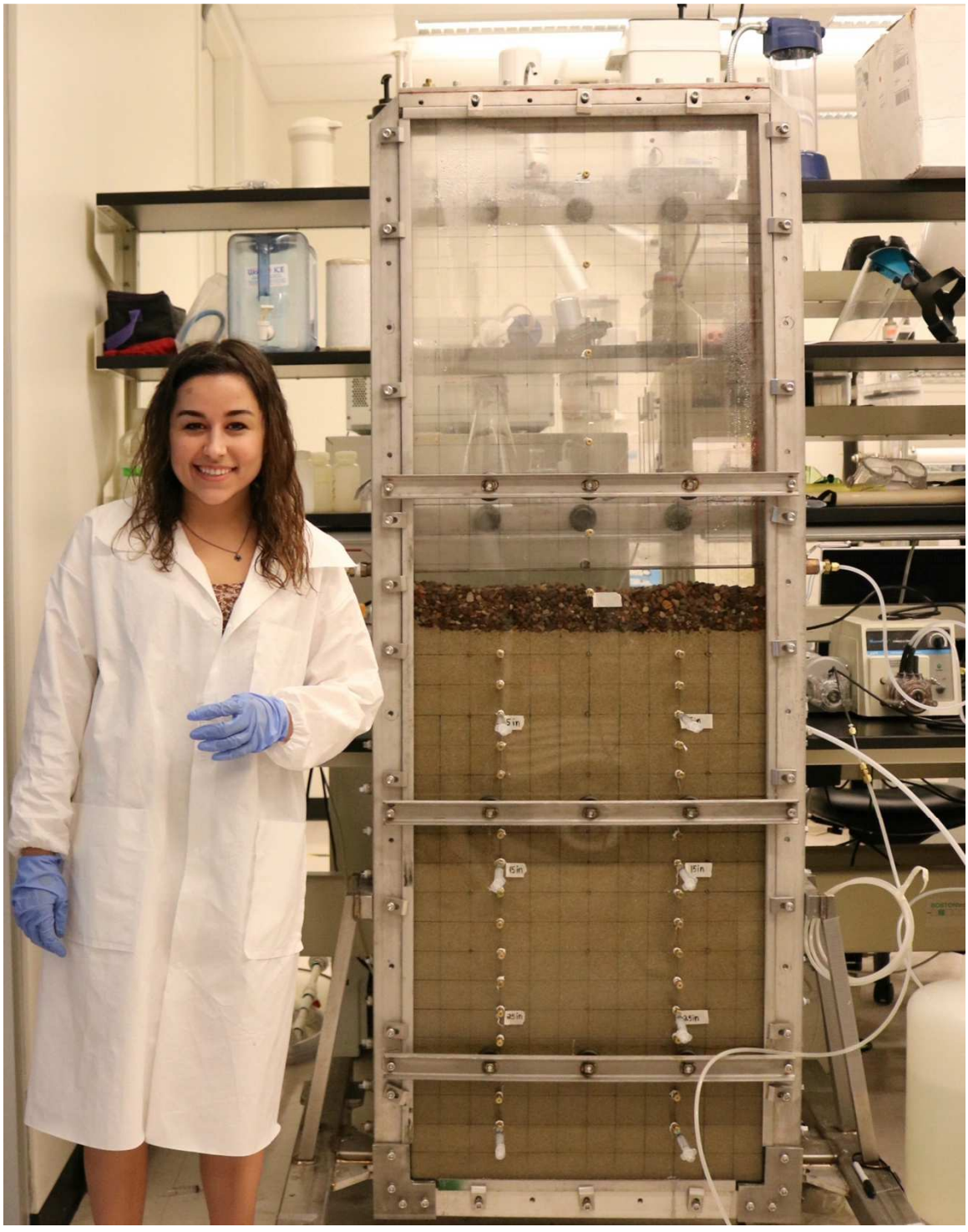

Figure C.1 Author with the Tank

Figure C.2 Sampling from Left 5 inch Port

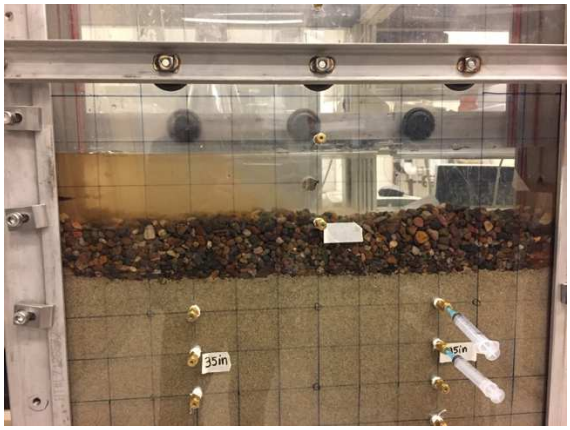

Figures C.3, C.4 Trapped Air Bubbles Released during High Flowrate Flushing

APPENDIX D

BACTERIA COLONY APPEARANCE MORPHOLOGY

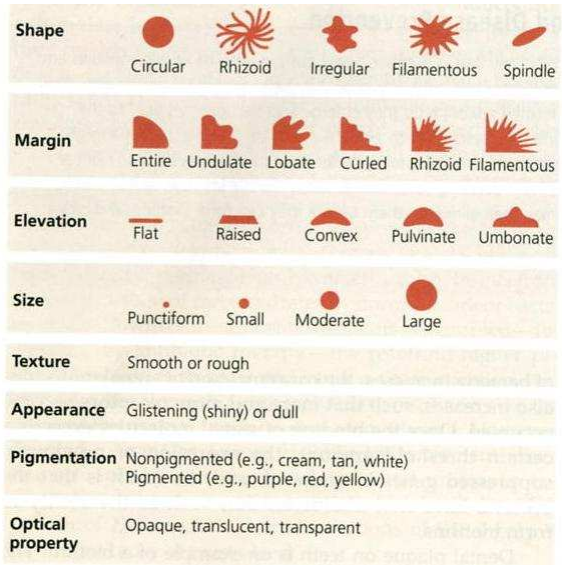

Figure D.1 Bacteria Colony Appearance Morphology Breakdown

***E. coli*, on TSA media**

Figure D.2 *E. coli* Streak Plate on TSA Media

Shape (form): circular
Margin: entire
Elevation: raised
Size: punctiform, small, moderate
Texture (surface): smooth
Appearance: shiny
Pigmentation: nonpigmented (colorless)

Optical property: translucent

***E. coli*, on Brilliance media**

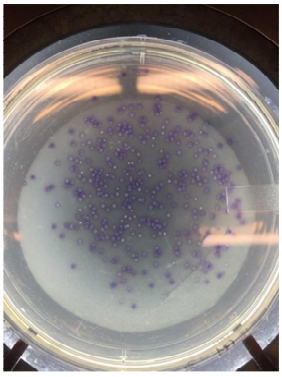

Figure D.3 *E. coli* Spread Plate on Brilliance Media

Shape (form): circular
Margin: entire
Elevation: raised
Size: punctiform, small
Texture (surface): smooth
Appearance: shiny
Pigmentation: Pigmented purple
Optical property: opaque

***Salmonella*, on TSA media**

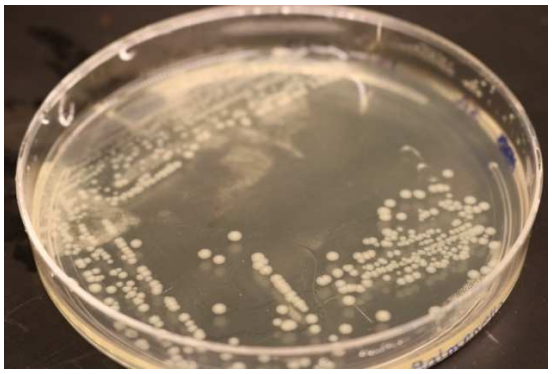

Figure D.4 *Salmonella* Streak Plate on Brilliance Media

Shape (form): circular

Margin: entire
Elevation: raised
Size: punctiform, small, moderate
Texture (surface): smooth
Appearance: shiny
Pigmentation: nonpigmented (colorless)
Optical property: translucent

APPENDIX E

DYE-TRACER TEST PHOTOS

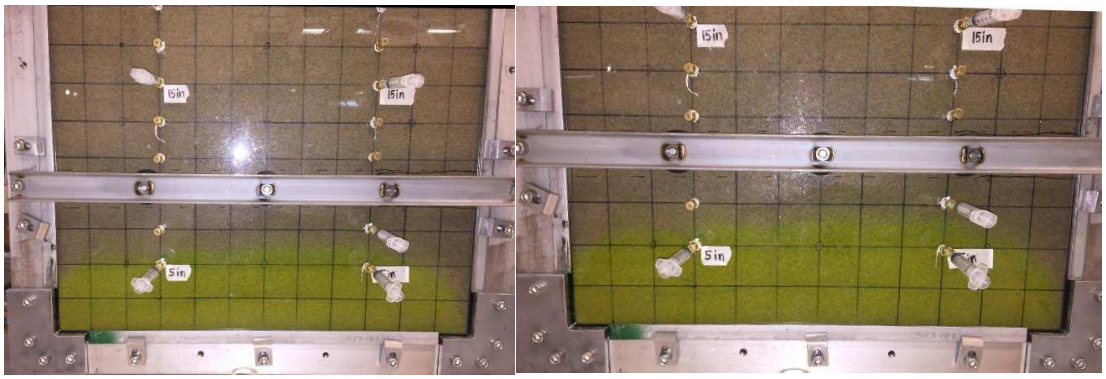

Figure 4.1 Dye Pattern on Media 14 Hours after Injection (left)

Figure E.1 Dye Pattern on Media 15 Hours after Injection (right)

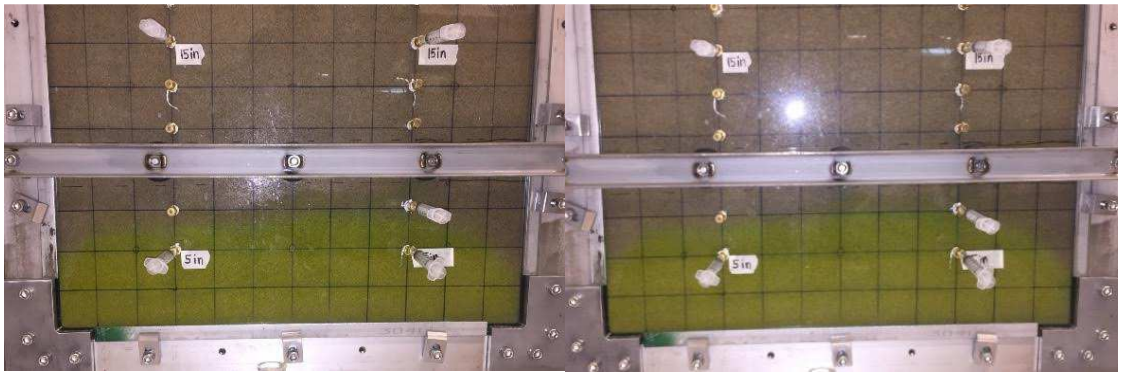

Figure E.2 Dye Pattern on Media 16 Hours after Injection (left)

Figure E.3 Dye Pattern on Media 17 Hours after Injection (right)

Figure 4.2 Dye Pattern on Media 18 Hours after Injection (right)

Figure E.4 Dye Pattern on Media 20 Hours after Injection (right)

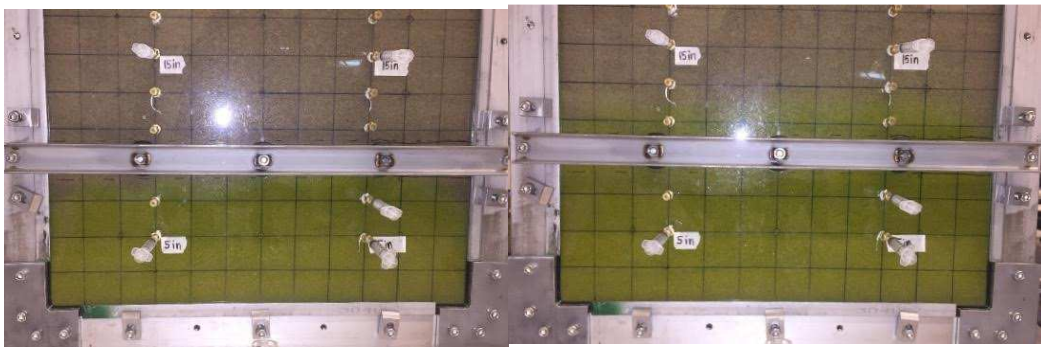

Figure 4.3 Dye Pattern on Media 22.5 Hours after Injection (left)

Figure 4.4 Dye Pattern on Media 34 Hours after Injection (right)

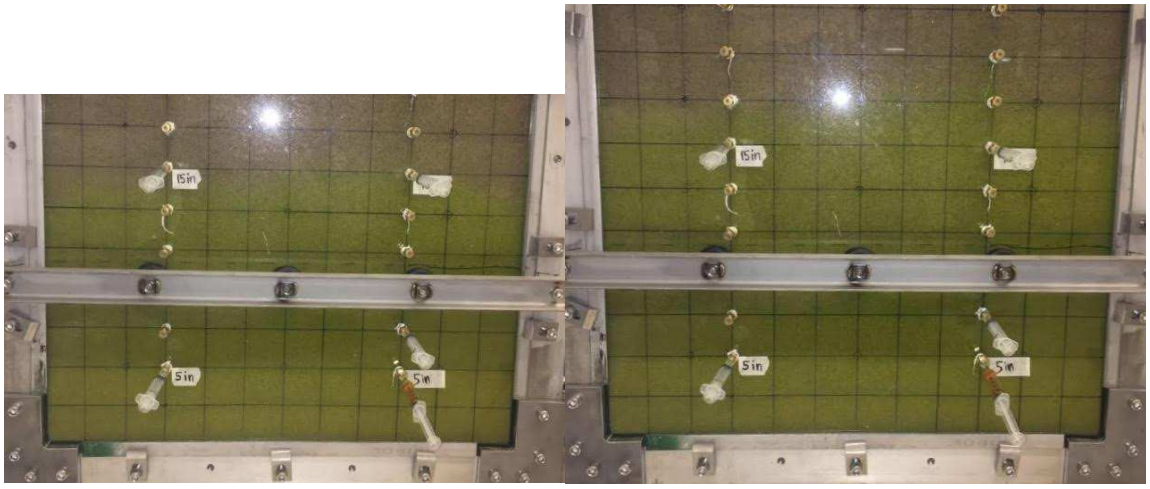

Figure E.5 Dye Pattern on Media 43.5 Hours after Injection (left)

Figure E.6 Dye Pattern on Media 45.5 Hours after Injection (right)

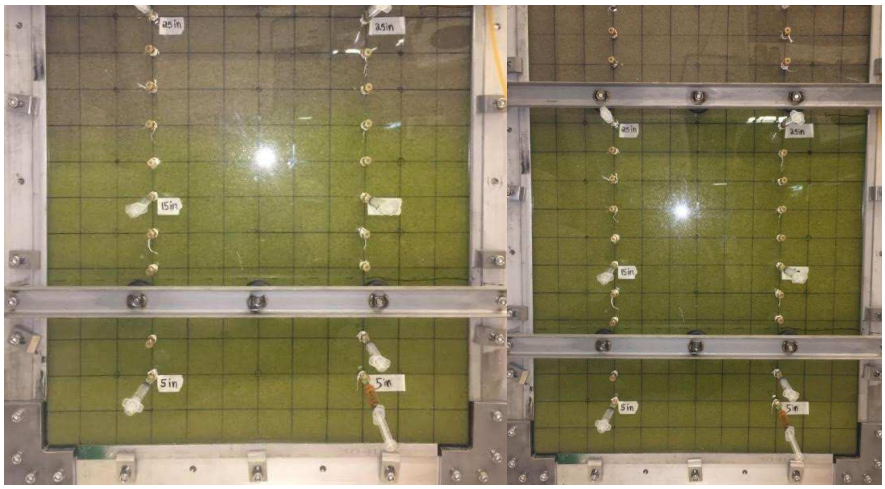

Figure 4.5 Dye Pattern on Media 49.5 Hours after Injection (left)

Figure 4.6 Dye Pattern on Media 66 Hours after Injection (right)

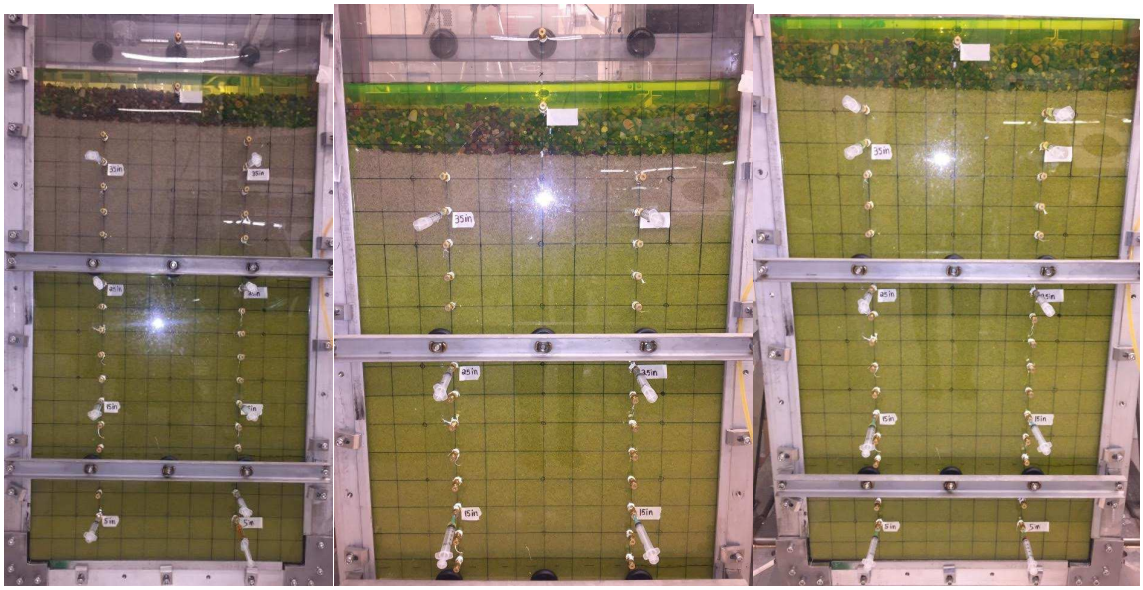

Figure E.7 Dye Pattern on Media 94.5 Hours after Injection (left)

Figure E.8 Dye Pattern on Media 108 Hours after Injection (middle)

Figure E.9 Dye Pattern on Media 120 Hours after Injection (right)